Analysis of the High Pressure Polyethylene Tubular Reactor with Axial Mixing

A theoretical study was carried out for the analysis of the high pressure polyethylene tubular reactor with axial mixing (TRAM). In the study, the Contraction Mapping Theorem in the square-integrable function space $L_2[0, 1]$ was first used to derive a uniqueness criterion for the existence of the steady state solution of the polyethylene TRAM. Then, an algorithm was derived which enabled us to compute the profiles of reactor temperature and concentration. Details of reactor performance were investigated in terms of the reactor operating and design variables: heat transfer coefficient, feed temperature and concentration, axial mixing, the length of reactor, and the distribution of preheating and cooling zones of the reactor. Also investigated in this study was the product quality in terms of the number-average molecular weight and molecular weight distribution as affected by change in reactor operating conditions and by the chain transfer reactions.

SATISH AGRAWAL

and

CHANG DAE HAN

Department of Chemical Engineering
Polytechnic Institute of New York
Brooklyn, New York 11201

SCOPE

The free-radical polymerization of ethylene at high pressure is a reaction of broad commercial and theoretical interest. In commercial practice, the high pressure process is undertaken in both autoclaves and tubular reactors. Earlier efforts in analyzing the steady state solutions of the high pressure polyethylene system have been directed either to the continuous stirred-tank reactor or to the ideal case of the tubular reactor, namely the plug flow reactor (Goldstein and Hwa, 1966; Hoftyzer and Zwietering, 1961; Volter, 1963). However, in the commercial operation of high pressure polyethylene tubular reactors, consideration of axial mixing is of practical importance. This is because a flow control valve located near the reactor exit is used to give periodic pulsation to prevent the rapid buildup of polymer scale on the reactor wall which would adversely affect the heat transfer coefficient. The pulsations increase axial mixing in the reactor and consequently influences the monomer conversion, temperature profile, and the product quality.

In the present paper, a theoretical study will be presented which analyzes the performance of the high pressure polyethylene tubular reactor including the effect of axial mixing. For the study, an abstract function space, the square-integrable function space $L_2[0, 1]$, was first introduced to derive a uniqueness criterion for the existence of the steady state solution of the system differential equations. Then, the resulting system integral equations were numerically solved by the use of a successive approximation scheme to obtain the profiles of monomer concentration and temperature in the reactor.

One of the most important problems encountered in operating a polymerization reactor is to control the product quality, namely the molecular weight and its distribution. Therefore it is of practical importance to develop a simulation model which can predict the product quality as affected by the reactor operating conditions. In the present paper, we shall present some predicted results for the product quality of polyethylene produced by means of a high pressure tubular reactor. Also discussed will be the effect of chain transfer reactions on the molecular weight and its distribution.

CONCLUSIONS AND SIGNIFICANCE

Mathematical formulations of chemical engineering systems are generally expressed in terms of nonlinear differential equations. The present study shows that transformation of the system differential equations into integral equations, and an investigation of the properties of the resulting integral operators in abstract function spaces, is very useful for the analysis of a complex chemical process, such as the high pressure process for making polyethylene in tubular reactors. The analysis can be of practical use for the design of new, and the optimum operation of existing, reactors. The salient feature of the function space method used in this study is that it provides not only a uniqueness criterion for the existence of the steady state solution, but also a simple computational algorithm (a successive approximation scheme).

The successive approximation scheme was used in conjunction with the uniqueness criterion to construct a region of steady states (range of system parameters for which reactor operation is stable) for several reactor variables. The following specific conclusions are drawn from the present study: (1) axial mixing affects both reactor performance and product quality (that is, the molecular weight and its distribution), (2) the chain transfer reactions broaden the molecular weight distribution, (3) the jacket fluid (coolant) temperature, feed temperature, and the overall heat transfer coefficient all have a profound effect on reactor performance (that is, concentration and temperature profiles), and (4) the initiator concentration affects reactor performance significantly.

Correspondence concerning this paper should be addressed to C. D. Han. S. Agrawal is with Polaroid Corporation, New Bedford, Massachusetts 02745.

Various processes for the polymerization of ethylene have been described by Albright (1974), Smith (1964), and Raff and Allison (1956). Commercially available polyethylene is manufactured either by the low pressure process which yields high density polyethylene, or by the high pressure process which yields low density polyethylene. The high pressure process can be undertaken by any one of the four common polymerization techniques, namely, bulk polymerization, solution polymerization, suspension polymerization, and emulsion polymerization. However, the bulk polymerization technique is the most common one commercially.

The bulk polymerization technique for the high pressure process requires a highly purified ethylene stream (99.9% ethylene). The process pressure ranges somewhere between 1000 and 3000 atm (Miles and Briston, 1965). The ethylene stream together with an initiator which generates free radicals enters into a reactor. Two main commercial reactor designs have evolved: the tubular reactor and the stirred autoclave reactor. The tubular reactor can be a long single tube, a tube with multiple feed streams along its length, or many tubes in parallel. Reactor temperature ranges somewhere between 100° and 300°C. Temperatures above 300°C are not used, primarily because decomposition of ethylene may occur above 300°C. The mixture of polymer and monomer leaving the reactor is separated by pressure reduction into monomer-rich and polymer-rich streams. The monomer-rich stream is either recycled to the reactor inlet or is used in a downstream process. The polymer-rich stream is usually further concentrated by a second separation step and then extruded into ribbons or strands for pelletizing. It should be noted that some commercial processes use oxygen as an initiator.

The initiation of the polymerization process requires primary free radicals. In the earlier days, oxygen was used almost exclusively (Ehrlich, Pittilo, and Cotman, 1958; Ehrlich and Pittilo, 1960). The modern trend, however, is to use organic initiators such as peroxides, hydroperoxides, etc. (Steiner et al., 1967). The temperature at which significant initiator decomposition rates occur is a function of the type of initiator. Hence, a successful operation of the reactor requires the proper selection of an initiator, or a combination of more than one initiator. The initiator can be injected directly into the reactor in the feed stream, or prior to monomer compression. The precise metering and control of the injection rate is essential since this can affect the polymerization rate significantly and hence the reactor temperature profile. Some manufacturers vary the initiator injection rate to control the reactor temperature, while others keep the injection rate fixed and control reactor temperature by manipulating the flow rate of coolant, for instance.

The high pressure polyethylene tubular reactor is characterized by its large length-to-diameter ratio which ranges somewhere from 250:1 to as high as 12000:1 (Smith, 1964). Heat is transferred from or to the reactor through its walls by the fluid circulating through the jacket that surrounds it. High jacket temperatures are used in the initial portion of the reactor to heat the cold feed to initiation temperature. Lower jacket temperatures are used in latter portion of the reactor in order to remove the heat of the reaction generated by the polymerization. It should be mentioned that poor control of reactor temperature can cause a polymer buildup on the reactor wall which, if not removed, can affect reactor performance significantly through a marked reduction in the heat transfer coefficient. A number of methods have been devised to correct this problem. One commonly used technique is to pulse the reactor flow at a controlled rate. It should be pointed out that the flow pulsation significantly increases axial mixing.

A number of researchers have made studies on the analysis of polymerization reactor systems. A majority of these studies focused on the continuous stirred-tank reactor (CSTR) (Goldstein and Hwa, 1966; Goldstein and Amundson, 1965; Zeman and Amundson, 1965; Warden and Amundson, 1962; Hoftyzer and Zwietering, 1961; Thies and Schoeneman, 1970), and relatively few on the tubular reactor (Mullikin et al., 1965; Cintron-Cordero et al., 1968).

The system equations characterizing the CSTR are a set of coupled nonlinear algebraic equations. Although free radical polymerization kinetics can make manipulation of the system equations quite cumbersome, these equations are amenable to solution by the usual iterative techniques (such as Newton-Raphson). Such techniques were used by Goldstein and Amundson (1965) for studying the effects on product properties of important reactor variables for the general free radical (addition) polymerization system, and by Goldstein and Hwa (1966) for the high pressure polyethylene system.

A stability analysis of the CSTR steady state for free radical addition polymerization systems has also been undertaken by several authors such as Hoftyzer and Zwietering (1961), Warden and Amundson (1962), Goldstein and Amundson (1965), and Goldstein and Hwa (1966). All of these studies have focused on the linearized version of the dynamic equations. Although such studies do provide valuable insight into the process, the problem of stability in the large is still to be tackled.

Mullikin et al. (1965) have investigated the effects on reactor conversion and temperature profile of selected reactor variables such as initiator concentration and jacket temperature for an idealized polyethylene tubular reactor, that is, a plug flow reactor. Steady state solutions were obtained by simulation on an analog computer. It should be pointed out, however, that their study does not adequately represent the industrial reactor because commercial polyethylene tubular reactors are pulsed periodically and are therefore subject to a high degree of axial mixing, which could have a marked effect on the product quality.

Volter (1963) has investigated the stability of the steady states for a polyethylene tubular (plug flow) reactor. This was done by deriving stability criteria for the mass and energy balance equations for a small segment of it. Volter contends that the stability criteria derived are valid for the entire reactor. Although a tubular reactor with axial mixing can be approximated by a finite number of cascaded CSTR's, in order for the results of a CSTR to be applicable to the entire cascade one has to relate the degree of mixing to each element in the cascade. Volter has assumed further that the concentration of the initiator is invariant. This is not the case in practical situations.

Control of the polyethylene reactor has to be such that not only are the polymer production rates uniform but also that the polymer properties such as density, molecular weight distribution, average molecular weight, etc. must be reproducible. Reactor variables that have a significant impact on the performance of the reactor can be listed as: (1) number and location of initiator feed points, (2) injection rate of initiator, (3) feed temperature, (4) jacket temperature, and (5) the frequency of pulsation of flow. Although specific details of the manner by which the above variables are manipulated are not known (since this is proprietary information), it is generally accepted that a close regulation of these variables is necessary. If this is not done, one can encounter runaway conditions in the reactor.

KINETICS OF ETHYLENE POLYMERIZATION

The theory of free radical polymerization (Flory, 1953; Bamford et al., 1958) was applied to develop mathematical expressions for the reaction rate. To describe the polymerization, a kinetic model was postulated which included seven types of reactions: initiator decomposition, chain initiation, propagation, termination by recombination, and radical transfer to monomer, polymer (long chain branching) and solvent. In the kinetic rate expressions given below, we made the following assumptions: (1) the rates of generation and termination of free-radicals are equal (the so-called "steady state" assumption); (2) the termination step is governed by recombination; (3) consumption of initiator free radicals by other reactions is negligible.

(i) The decomposition rate of initiator:

$$R_d = -k_d C_I \tag{1}$$

(ii) The chain initiation rate:

$$R_i = 2k_{d\epsilon} C_I \tag{2}$$

(iii) The monomer consumption rate (that is, the overall polymerization rate)

$$R_M = \left\{ \frac{(k_p)^2 k_{d\epsilon}}{k_{tc}} \right\}^{1/2} C_I^{1/2} C_M \tag{3}$$

The total reaction rate for dead polymer $\sum_{r=2}^{\infty} R_{M_r}$ which will be used later for computing the average molecular weight of the product is given by (Agrawal, 1974)

$$\sum_{r=2}^{\infty} R_{M_r} = \Phi_4 - \{k_T + k_{tr,P} Q_0\} C_{M_1^*} \tag{4}$$

where

$$\Phi_4 = Q_0^* \{k_{tc} Q_0^* + k_T\} \tag{5}$$

in which

$$k_T = k_{tr,S} C_S + k_{tr,M} C_M \tag{6}$$

and

$$C_{M_1^*} = [2k_{tc}(Q_0^*)^2 + k_T Q_0^*]/\nu \tag{7}$$

Note in Equation (7) that ν and Q_0^* are given by

$$\nu = 2k_{tc}Q_0^* + k_T + k_{tr,P}Q_0 + k_P C_M \tag{8}$$

and

$$Q_0 = \left(\frac{k_{d\epsilon} C_I}{k_{tc}} \right)^{1/2} \tag{9}$$

respectively.

It should be noted that the reaction rate constants are generally dependent on both temperature and pressure. As pointed out by Shrier et al. (1965), in a rigorous sense the temperature and pressure dependence of rate constants should be expressed in terms of energies and volume of changes of activation. Using kinetic data reported in the literature, we have obtained expressions for various rate constants (Agrawal, 1974). A summary of the rate expressions is given in Table 1.

Table 1. A Summary of Rate Constant Correlation

Initiator decomposition	$k_d = (k_d)_0 \exp\left(\frac{-\hat{E}_d(P)}{RT}\right)$ (1/s)	$(k_d)_0$	$\hat{E}_d(P) = E_d + 0.170P$ (cal/g-mole)
Chain initiation	$k_d = (k_{d\epsilon})_0 \exp\left(\frac{-\hat{E}_i(P)}{RT}\right)$ (1/s)	$(k_{d\epsilon})_0 = 0.75\,(k_d)_0$	$\hat{E}_i(P) = \hat{E}_d(P)$ (cal/g-mole)
Chain propagation	$k_p = (k_p)_0 \exp\left(\frac{-\hat{E}_p(P)}{RT}\right)$ $\left(\frac{\text{liters}}{\text{g-mole s}}\right)$	$(k_p)_0 = 1.25 \times 10^8$	$\hat{E}_p(P) = 7800 + 0.5P$ (cal/g-mole)
Chain termination	$k_{tc} = (k_{tc})_0 \exp\left(\frac{-\hat{E}_{tc}(P)}{RT}\right)$ $\left(\frac{\text{liters}}{\text{g-mole s}}\right)$	$(k_{tc})_0 = 2.2 \times 10^{10}$	$\hat{E}_{tc}(P) = 1000 + 0.244P$ (cal/g-mole)
Chain transfer to dead polymer	$k_{tr,p} = (k_{tr,p})_0 \exp\left(\frac{-\hat{E}_{tr,p}(P)}{RT}\right)$ $\left(\frac{\text{liters}}{\text{g-mole s}}\right)$	$(k_{tr,p}) = k^0_{tr,p} \exp\left(\frac{12000}{RT^0}\right)$	$\hat{E}_{tr,p}(P) = 12000$ (cal/g-mole)
Chain transfer to monomer	$k_{tr,M} = (k_{tr,M})_0 \exp\left(\frac{-\hat{E}_{tr,M}(P)}{RT}\right)$ $\left(\frac{\text{liters}}{\text{g-mole s}}\right)$	$(k_{tr,M})_0 = k^0_{tr,M} \exp\left(\frac{12000}{RT^0}\right)$	$\hat{E}_{tr,M}(P) = 12000$ (cal/g-mole)
Chain transfer to modifier	$k_{tr,S} = (k_{tr,S})_0 \exp\left(\frac{-\hat{E}_{tr,S}(P)}{RT}\right)$ $\left(\frac{\text{liters}}{\text{g-mole s}}\right)$	$(k_{tr,S})_0 = k^0_{tr,S} \exp\left(\frac{12000}{RT^0}\right)$	$\hat{E}_{tr,S}(P) = 12000$ (cal/g-mole)

Note: Values of $(k_d)_0$ and E_d are given in Table 2.

SYSTEM EQUATIONS FOR THE HIGH-PRESSURE POLYETHYLENE TUBULAR REACTOR WITH AXIAL MIXING (TRAM)

The differential equations representing the mathematical model of the polyethylene tubular reactor with axial mixing are presented. These differential equations will be transformed into integral equations, which will then be analyzed in the square-integrable function space $L_2[0, 1]$ to derive both a uniqueness criterion and algorithms for numerical computations.

Mass and Energy Balance

The steady state mass and energy balance of the TRAM for the polymerization of ethylene may be written as

(i) Mass balance for initiator

$$\hat{D}_I \frac{d^2C_I}{dx^2} - v\frac{dC_I}{dx} - C_I(k_d)_0 \exp\left(\frac{-\hat{E}_d(P)}{RT}\right) = 0 \tag{10}$$

(ii) Mass balance for monomer

$$\hat{D}_M \frac{d^2C_M}{dx^2} - v\frac{dC_M}{dx} - \left\{\frac{(k_p)_0^2\,(k_d\epsilon)_0}{(k_{tc})_0}\exp\left(\frac{-\hat{E}_{\text{pol}}(P)}{RT}\right)\right\}^{1/2} C_I^{1/2}\,C_M = 0 \tag{11}$$

(iii) Energy balance

$$\hat{K}_L \frac{d^2T}{dx^2} - \rho C_p\, v\frac{dT}{dx} + (-\Delta H_p)\left\{\frac{(k_p)_0^2\,(k_d\epsilon)_0}{(k_{tc})_0}\exp\left(\frac{-\hat{E}_{\text{pol}}(P)}{RT}\right)\right\}^{1/2} C_I^{1/2}\,C_M + (-\Delta H_d)\,(k_d)_0 C_I \exp\left(\frac{-\hat{E}_d(P)}{RT}\right) - \frac{4U}{D}(T - T_c) = 0 \tag{12}$$

together with the boundary conditions:

(i) At the tube entrance ($x = 0$):

$$v((C_I)_0 - C_I)]_{x=0} = -\hat{D}_I \frac{dC_I}{dx}\Big]_{x=0} \tag{13}$$

$$v((C_M)_0 - C_M)]_{x=0} = -\hat{D}_M \frac{dC_M}{dx}\Big]_{x=0} \tag{14}$$

$$\rho v C_p(T_0 - T)]_{x=0} = -\hat{K}_L \frac{dT}{dx}\Big]_{x=0} \tag{15}$$

(ii) At the tube exit ($x = L$)

$$\frac{dC_I}{dx}\Big]_{x=L} = 0;\quad \frac{dC_M}{dx}\Big]_{x=L} = 0;\quad \frac{dT}{dx}\Big]_{x=L} = 0 \tag{16}$$

The above equations can easily be derived by starting with the fundamental equations of change (see, for example, Levenspiel, 1962; Aris, 1965; Smith, 1970) and by using the reaction rate expressions. Implicit in writing Equations (10) to (16) is the assumption that the reacting system is homogeneous (that is, a single phase).

Note that in Equation (12) the heat effects due to the chain initiation and termination steps are neglected. Note further that the use of the steady state assumption for free-radicals has enabled us to eliminate the intermediate species (free radicals) from the basic mass and energy balance equation.

Introducing new dimensionless variables (see Notation), Equations (10) to (16) may be rewritten as

$$\frac{1}{Pe_I}\frac{d^2y_1}{dz^2} - \frac{dy_1}{dz} + f_1(y_1, y_3) = 0 \tag{17}$$

$$\frac{1}{Pe_M}\frac{d^2y_2}{dz^2} - \frac{dy_2}{dz} + f_2(y_1, y_2, y_3) = 0 \tag{18}$$

$$\frac{1}{Pe_H}\frac{d^2y_3}{dz^2} - \frac{dy_3}{dz} - \beta y_3 + f_3(y_1, y_2, y_3) = 0 \tag{19}$$

together with boundary conditions

$$Pe_I y_1(0) = \frac{dy_1}{dz}\Big]_{z=0} \tag{20}$$

$$Pe_M y_2(0) = \frac{dy_2}{dz}\Big]_{z=0} \tag{21}$$

$$Pe_H y_3(0) = \frac{dy_3}{dz}\Big]_{z=0} \tag{22}$$

$$\frac{dy_1}{dz}\Big]_{z=1} = 0;\quad \frac{dy_2}{dz}\Big]_{z=1} = 0;\quad \frac{dy_3}{dz}\Big]_{z=1} = 0 \tag{23}$$

in which f_1, f_2, and f_3 are defined by

$$f_1(y_1, y_3) = Da_I\,(1 - y_1)\exp\left(\frac{y_3}{1 + \epsilon_1 y_3}\right) \tag{24}$$

$$f_2(y_1, y_2, y_3) = (1 - y_2)\left\{Da_M(1 - y_1)\exp\left(\frac{\epsilon_2 y_3}{1 + \epsilon_1 y_3}\right)\right\}^{1/2} \tag{25}$$

$$f_3(y_1, y_2, y_3) = B_1 f_1(y_1, y_3) + B_2 f_2(y_1, y_2, y_3) + \beta y_c \tag{26}$$

Expressions for the Molecular Weight of the Product

The polymer product consists of a mixture of similar species, each having different molecular weights. It is customary to represent the molecular weight of a polymer in terms of the number- and weight-average molecular weight.

If the nth moment of a polymer is defined by the equation

$$Q_n = \sum_{r=2}^{\infty} r^n C_{M_r} \tag{27}$$

the number- and weight-average molecular weight are given by

$$\overline{M}_n = \frac{28Q_1}{Q_0} \tag{28}$$

and

$$\overline{M}_w = \frac{28Q_2}{Q_1} \tag{29}$$

respectively, in which 28 is the molecular weight of ethylene. It can be seen then that the computation of the average molecular weights requires the determination of the zeroth (Q_0), first (Q_1), and second moments (Q_2) of the dead polymer.

Now, the mass balance equation for dead polymer M_r ($r = 2, \infty$) can be expressed by

$$\hat{D}_{M_r}\frac{d^2C_{M_r}}{dx^2} - v\frac{dC_{M_r}}{dx} + R_{M_r} = 0 \tag{30}$$

together with the boundary conditions

$$((C_{M_r})_0 - C_{M_r})]_{x=0} = -\hat{D}_{M_r} \left.\frac{dC_{M_r}}{dx}\right|_{x=0} \quad (31)$$

$$\left.\frac{dC_{M_r}}{dx}\right]_{x=L} = 0 \quad (32)$$

If Equations (30) to (32) are multiplied by r^n and summed from $r = 2$ to $r = \infty$, one has

$$\hat{D}_{M_r} \frac{d^2Q_n}{dx^2} - v\frac{dQ_n}{dx} + \sum_{r=2}^{\infty} r^n R_{M_r} = 0 \quad (33)$$

together with the boundary conditions

$$\left[\sum_{r=2}^{\infty} r^n (C_{M_r})_0 - Q_n\right]\Bigg|_{x=0} = -\hat{D}_{M_r} \left.\frac{dQ_n}{dx}\right|_{x=0} \quad (34)$$

$$\left.\frac{dQ_n}{dx}\right|_{x=L} = 0 \quad (35)$$

The solution of Equation (33) will yield the desired moments for $n = 0$, 1 and 2. Note that, in writing Equations (33) to (35), it is assumed that the empirical axial diffusivity $\hat{D}_{M_r}$ is independent of chain length.

The overall reaction rate for dead polymer $\sum_{r=2}^{\infty} R_{M_r}$ in Equation (33) for $n = 0$ is given by Equation (4). The first and second moments

$$\left[\sum_{r=2}^{\infty} r R_{M_r}\right] \text{ and } \left[\sum_{r=2}^{\infty} r^2 R_{M_r}\right]$$

of the dead polymer are given by (Agrawal, 1974):

$$\sum_{r=2}^{\infty} r R_{M_r} = \Phi_5 \quad (36)$$

and

$$\sum_{r=2}^{\infty} r^2 R_{M_r} = \Phi_6 \quad (37)$$

in which Φ_5 and Φ_6 are defined by

$$\Phi_5 = 2k_{tc}(Q_0^*)^2 + Q_0^*(k_pC_M + k_T) - (k_T + k_{tr,P}Q_0)C_{M_1^*} \quad (38)$$

and

$$\Phi_6 = 2k_{tc}((Q_1^*)^2 + (Q_0^*)^2) + Q_0^*(k_PC_M + k_T) + 2k_PC_MQ_1^* - (k_T + k_{tr,P}Q_0)\,C_{M_1^*} \quad (39)$$

Note that Q_0^* is given by Equation (9) and Q_1^* which is the first moment of total free radical concentration, is given by

$$Q_1^* = \frac{2k_{tc}(Q_0^*)^2 + Q_0^*(k_pC_M + k_T + k_{tr,P}Q_1)}{(v - k_pC_M)} \quad (40)$$

Introducing new dimensionless variables (see Notation), Equations (33) to (35) can be rewritten as

For $n = 0$,

$$\frac{1}{Pe_{M_r}}\frac{d^2y_4}{dz^2} - \frac{dy_4}{dz} + \frac{L}{v}\frac{\Phi_4(z)}{(C_4)_0} + f_4(y_4) = 0 \quad (41)$$

in which $f_4(y_4)$ is defined by

$$f_4(y_4) = \frac{L}{v(C_4)_0}(k_T + (C_4)_0\,k_{tr,P}\,(1 - y_4))C_{M_1^*} \quad (42)$$

For $n = 1$,

$$\frac{1}{Pe_{M_r}}\frac{d^2y_5}{dz^2} - \frac{dy_5}{dz} + \frac{L}{v}\frac{\Phi_5(z)}{(C_5)_0} = 0 \quad (43)$$

for $n = 2$,

$$\frac{1}{Pe_{M_r}}\frac{d^2y_6}{dz^2} - \frac{dy_6}{dz} + \frac{L}{v}\frac{\Phi_6(z)}{(C_6)_0} = 0 \quad (44)$$

Also, boundary conditions (34) and (35) may be rewritten as

For $n = 0$,

$$Pe_{M_r}\,y_4(0) = \left.\frac{dy_4}{dz}\right]_{z=0};\quad \left.\frac{dy_4}{dz}\right]_{z=1} = 0 \quad (45)$$

for $n = 1$,

$$Pe_{M_r}\,y_5(0) = \left.\frac{dy_5}{dz}\right]_{z=0};\quad \left.\frac{dy_5}{dz}\right]_{z=1} = 0 \quad (46)$$

for $n = 2$,

$$Pe_{M_r}\,y_6(0) = \left.\frac{dy_6}{dz}\right]_{z=0};\quad \left.\frac{dy_6}{dz}\right]_{z=1} = 0 \quad (47)$$

Transformation of System Differential Equations into Integral Equations

In order to apply the Contraction Mapping Theorem to Equations (17) to (19) and to Equations (41) to (44) for obtaining a uniqueness criterion and numerical algorithms for computing the steady state solutions, it is essential to transform the differential equations into integral equations. However, before this transformation is undertaken, we shall introduce the following transformations:

$$\hat{y}_1(z) = \exp(-Pe_I\,z/2)\,y_1(z) \quad (48)$$

$$\hat{y}_2(z) = \exp(-Pe_M\,z/2)\,y_2(z) \quad (49)$$

$$\hat{y}_3(z) = \exp(-Pe_H\,z/2)\,y_3(z) \quad (50)$$

$$\hat{y}_{n+3}(z) = \exp(-Pe_{M_r}\,z/2)y_{n+3}(z);\quad (n = 1, 2, 3) \quad (51)$$

This is done merely for convenience in solving an associated eigenvalue problem (Han and Agrawal, 1973) which will arise in the subsequent analysis.

Then the integral representation of Equations (17) to (19), and Equations (41) to (44) may be given by

$$\hat{y}_i = \hat{A}_i\,\hat{y}_i \quad (i = 1, 2, 3, 4, 5, 6) \quad (52)$$

where $\hat{A}_i$ are integral operators defined by (Han and Agrawal, 1973):

$$\hat{A}_i\,y_i = \int_0^1 \hat{k}_i(z, \xi)\,\hat{f}_i(\xi, y_1, y_2, y_3, y_4, y_5, y_6)d\xi \quad (i = 1, 2, 3, 4, 5, 6) \quad (53)$$

in which

$$\hat{f}_1(z, y_1, y_3) = Pe_I \exp(-Pe_I\,z/2)\,f_1(y_1, y_3) \quad (54)$$

$$\hat{f}_2(z, y_1, y_2, y_3) = Pe_M \exp(-Pe_M\,z/2)\,f_2(y_1, y_2, y_3) \quad (55)$$

$$\hat{f}_3(z, y_1, y_2, y_3) = Pe_H \exp(-Pe_H\,z/2)\,f_3(y_1, y_2, y_3) \quad (56)$$

$$\hat{f}_4(z, y_4) = Pe_{M_r} \exp(-Pe_{M_r} z/2) \left\{ \frac{L}{v} \frac{\Phi_4(z)}{(C_4)_0} + f_4(y_4) \right\} \quad (57)$$

$$\hat{f}_5(z, y_4) = Pe_{M_r} \exp(-Pe_{M_r} z/2) \left\{ \frac{L}{v} \frac{\Phi_5(z, y_4)}{(C_5)_0} \right\} \quad (58)$$

$$\hat{f}_6(z, y_4) = Pe_{M_r} \exp(-Pe_{M_r} z/2) \left\{ \frac{L}{v} \frac{\Phi_6(z, y_4)}{(C_6)_0} \right\} \quad (59)$$

It should be noted that Φ_5 and Φ_6 depend on y_4. Note that $\hat{k}_i(z, \xi)$ ($i = 1$ to 6) in Equation (53) are the kernels of the integral operators $\hat{A}_i$ ($i = 1, \ldots, 6$) and they are given by

$$\hat{k}_1(z, \xi) = \frac{1}{Pe_I} [\exp(Pe_I(\xi - z)/2)\, H(z - \xi) + \exp(Pe_I(z - \xi)/2)\, H(\xi - z)] \quad (60)$$

$$\hat{k}_2(z, \xi) = \frac{1}{Pe_M} [\exp(Pe_M(\xi - z)/2)\, H(z - \xi) + \exp(Pe_M(z - \xi)/2)\, H(\xi - z)] \quad (61)$$

$$\hat{k}_3(z, \xi) = \frac{\left\{ e^{bz} - \frac{a-b}{a+b} e^{-b} \right\} \left\{ e^{b\xi} - \frac{a-b}{a+b} e^{b(2-\xi)} \right\} H(\xi - z)}{2b \left\{ \frac{a+b}{a-b} e^{2b} - \frac{a-b}{a+b} \right\}} + \frac{\left[e^{b\xi} - \frac{a-b}{a+b} e^{-b} \right] \left[e^{bz} - \frac{a-b}{a+b} e^{b(2-z)} \right] H(z - \xi)}{2b \left\{ \frac{a+b}{a-b} e^{2b} - \frac{a-b}{a+b} \right\}} \quad (62)$$

$$\hat{k}_{n+3}(z, \xi) = \frac{1}{Pe_{M_r}} [\exp(Pe_{M_r}(\xi - z)/2)\, H(z - \xi) + \exp(Pe_{M_r}(z - \xi)/2)\, H(\xi - z)]; \quad (n = 1, 2, 3) \quad (63)$$

in which $H(\xi - z)$ is the Heaviside unit function and

$$a = Pe_H/2 \quad (64)$$

$$b = \left(\frac{Pe_H^2}{4} + Pe_H \beta \right)^{1/2} \quad (65)$$

Readers who are not familiar with the use of integral operators may consult the standard textbooks (Coddington and Levinson, 1955; Friedman, 1956).

STEADY STATE SOLUTION AND ITS UNIQUENESS FOR THE POLYETHYLENE TRAM SYSTEM EQUATIONS

We now present an analysis which shows that the steady state solutions of the system Equation (52) exist and that they are unique. This is done by using an analytical tool very similar to that presented in an earlier paper by Han and Agrawal (1973), who then considered a simple chemical reaction: $A \rightarrow B$. In the present paper, however, expressions are developed which permit us to compute not only the profiles of reaction temperature and concentration, but also the average molecular weight (number- and weight-average) profiles.

Uniqueness Criterion of Steady State Solution

For $i = 1$, 2 and 3, Equation (52) represents the mass and energy balance of the polyethylene TRAM, which may be written as

$$\hat{\mathbf{Y}} = \hat{\mathbf{A}}\, \hat{\mathbf{Y}} \quad (66)$$

where

$$\hat{\mathbf{Y}} = \begin{bmatrix} \hat{y}_1 \\ \hat{y}_2 \\ \hat{y}_3 \end{bmatrix} \quad (67)$$

and

$$\hat{\mathbf{A}} = \begin{bmatrix} \hat{A}_1 & 0 & 0 \\ 0 & \hat{A}_2 & 0 \\ 0 & 0 & \hat{A}_3 \end{bmatrix} \quad (68)$$

in which the integral operators $\hat{A}_i$ ($i = 1, 2, 3$) are defined by Equation (53).

We shall derive below the conditions for which the operator $\hat{\mathbf{A}}$ is a contraction mapping in the function space $L_{2,3}[0, 1]$. Application of the Contraction Mapping Theorem will then yield a uniqueness criterion for the solution of Equation (66).

In order to show that the operator $\hat{\mathbf{A}}$ is a contraction mapping, one has to first show that $\hat{\mathbf{A}}$ maps the function $L_{2,3}$ into itself. The norm (in the function space $L_{2,3}[0, 1]$) of the measurable function $\hat{\mathbf{Y}}$, defined by Equation (66), is given by

$$\| \hat{\mathbf{A}}\, \hat{\mathbf{Y}} \|^2_{L_{2,3}} = \int_0^1 (\hat{\mathbf{A}}\, \hat{\mathbf{Y}})^T (\hat{\mathbf{A}}\, \hat{\mathbf{Y}})\, dz \quad (69)$$

Using Equations (68) and (53), Equation (69) can be rewritten as

$$\| \hat{\mathbf{A}}\, \hat{\mathbf{Y}} \|^2_{L_{2,3}} = \int_0^1 \sum_{i=1}^{3} \left[\int_0^1 \hat{k}_i(z, \xi)\, \hat{f}_i(\xi, y_1, y_2, y_3)\, d\xi \right]^2 dz \quad (70)$$

We shall show below that the integral operator $\hat{\mathbf{A}}$ maps the space $L_{2,3}$ into itself. For this, we first observe that the functions $f_i(y_1, y_2, y_3)$ ($i = 1, 2, 3$), which are defined by Equations (24) to (26), satisfy the following inequalities:

$$|f_1(y_1, y_3) - f_1(\psi_1, \psi_3)| \leq N_{1,1} |y_1 - \psi_1| + N_{1,3} |y_3 - \psi_3| \quad (71)$$

$$|f_2(y_1, y_2, y_3) - f_2(\psi_1, \psi_2, \psi_3)| \leq N_{2,1} |y_1 - \psi_1| + N_{2,2} |y_2 - \psi_2| + N_{2,3} |y_3 - \psi_3| \quad (72)$$

$$|f_3(y_1, y_2, y_3) - f_3(\psi_1, \psi_2, \psi_3)| \leq \left(\sum_{i=1}^{2} |B_i N_{i,1}| \right) |y_1 - \psi_1| + B_2 N_{2,2} |y_2 - \psi_2| + \left(\sum_{i=1}^{2} |B_i N_{i,3}| \right) |y_3 - \psi_3| \quad (73)$$

where

$$N_{i,j} = \sup_{y_1 \in L_{2,1}} \left| \frac{\partial f_i}{\partial y_j} \right|; \quad (i = 1,2; \quad j = 1, 2, 3) \quad (74)$$

If we now define $N_{\max,i}$ ($i = 1, 2, 3$) by

$$N_{\max,1} = \text{Max}\ (N_{1,1}, N_{1,3}) \tag{75}$$

$$N_{\max,2} = \text{Max}\ (N_{2,1}, N_{2,2}, N_{2,3}) \tag{76}$$

$$N_{\max,3} = \text{Max}\left[\sum_{i=1}^{2} |B_i N_{i,1}|, B_2 N_{2,2}, \sum_{i=1}^{2} |B_i N_{i,3}\right] \tag{77}$$

Inequalities (71) to (73) can be rewritten as

$$|f_1(y_1, y_3) - f_1(\psi_1, \psi_3)| \leq N_{\max,1}\,[|y_1 - \psi_1| + |y_3 - \psi_3|] \tag{78}$$

$$|f_2(y_1, y_2, y_3) - f_2(\psi_1, \psi_2, \psi_3)| \leq N_{\max,2}\left[\sum_{j=1}^{3} |y_j - \psi_j|\right] \tag{79}$$

$$|f_3(y_1, y_2, y_3) - f_3(\psi_1, \psi_2, \psi_3)| \leq N_{\max,3}\left[\sum_{j=1}^{3} |y_j - \psi_j|\right] \tag{80}$$

In order to show that Inequalities (78) to (80) are bounded in the space $L_{2,1}[0, 1]$, we examine the boundedness of the partial derivatives of the functions f_i ($i = 1, 2, 3$). Using Equation (74) and Equations (24) to (26), it can be shown that

$$N_{1,1} = \sup_{y_3 \in L_{2,1}} \left[Da_I \exp\left(\frac{y_3}{1 + \epsilon_1 y_3}\right)\right] \leq Da_I \exp\left(\frac{\hat{P}}{1 + \epsilon_1 \hat{P}}\right) \tag{81}$$

$$N_{1,3} = \sup_{y_1, y_3 \in L_{2,1}} \left[\frac{Da_I(1 - y_1)}{(1 + \epsilon_1 y_3)^2} \exp\left(\frac{y_3}{1 + \epsilon_1 y_3}\right)\right] \leq Da_I \exp\left(\frac{\hat{P}}{1 + \epsilon_1 \hat{P}}\right) \tag{82}$$

$$N_{2,1} = \sup_{y_1, y_2, y_3 \in L_{2,1}} \left[\left[\frac{Da_M \exp\left(\frac{\epsilon_2 y_3}{1 + \epsilon_1 y_3}\right)}{2(1 - y_1)}\right]^{1/2} (1 - y_2)\right] \leq \sup_{y_1 \in L_{2,1}} \left[\frac{Da_M \exp\left(\frac{\epsilon_2 \hat{P}}{1 + \epsilon_1 \hat{P}}\right)}{2(1 - y_1)}\right]^{1/2} \tag{83}$$

$$N_{2,2} = \sup_{y_1, y_3 \in L_{2,1}} \left\{\left[Da_M(1 - y_1) \exp\left(\frac{\epsilon_2 y_3}{1 + \epsilon_1 y_3}\right)\right]\right\} \leq Da_M \exp\left(\frac{\epsilon_2 \hat{P}}{1 + \epsilon_1 \hat{P}}\right) \tag{84}$$

$$N_{2,3} = \sup_{y_1, y_2, y_3 \in L_{2,1}} \left\{\left[\frac{Da_M(1 - y_1) \exp\left(\frac{\epsilon_2 y_3}{1 + \epsilon_1 y_3}\right)\epsilon_2}{(1 + \epsilon_1 y_3)^2}\right]^{1/2} (1 - y_2)\right\} \leq \left[Da_M(1 - y_1) \exp\left(\frac{\epsilon_2 \hat{P}}{1 + \epsilon_1 \hat{P}}\right) \epsilon_2\right]^{1/2} \tag{85}$$

where $\hat{P}$ is given by

$$\sup_{0 \leq z \leq 1} y_3(z) \leq \hat{P} < \infty \tag{86}$$

Now if y_1 is such that

$$\sup_{0 \leq z \leq 1} y_1(z) < 1 \tag{87}$$

is satisfied (that is, the consumption of the initiator is less than 100%), it can be shown that the partial derivatives of the functions f_i ($i = 1, 2, 3$) are bounded, that is, the inequality

$$N_{i,j} < \infty; \quad (i = 1, 2; \quad j = 1, 2, 3) \tag{88}$$

is satisfied. Further, since the kernels $\hat{k}_i(z, \xi)$ are continuous in z and ξ [see Equations (60) to (63)], it can be shown that the norm of $\hat{\mathbf{A}}\,\hat{\mathbf{Y}}$ is bounded, that is,

$$||\hat{\mathbf{A}}\,\hat{\mathbf{Y}}||^2_{L_{2,3}} < \infty \tag{89}$$

for all $\hat{\mathbf{Y}} \in L_{2,3}$. That is, the operator $\hat{\mathbf{A}}$ maps the space $L_{2,3}$ into itself.

Having shown that $||\hat{\mathbf{A}}\,\hat{\mathbf{Y}}||^2$ is finite, one can show further that the norm of $(\hat{\mathbf{A}}\,\hat{\mathbf{Y}} - \hat{\mathbf{A}}\,\hat{\Psi})$ is bounded also (Agrawal, 1974). That is,

$$||\hat{\mathbf{A}}\,\hat{\mathbf{Y}} - \hat{\mathbf{A}}\,\hat{\Psi}||^2_{L_{2,3}} \leq (\alpha_1)^2\,||\hat{\mathbf{Y}} - \hat{\Psi}||^2_{L_{2,3}} \tag{90}$$

where α_1 is defined by

$$\alpha_1 = [2(Pe_I N_{\max,1} \hat{N}_1 \mu_1^I)^2 + 3(Pe_M N_{\max,2} \hat{N}_2 \mu_1^{II})^2 + 3(Pe_H N_{\max,3} \hat{N}_3 \mu_1^{III})^2]^{1/2} \tag{91}$$

in which

$$\mu_1^I = \frac{1}{\frac{(Pe_I)^2}{4} + a_1(Pe_I)}; \quad a_1(Pe_I) > 0 \tag{92}$$

$$\mu_1^{II} = \frac{1}{\frac{(Pe_M)^2}{4} + a_2(Pe_M)}; \quad a_2(Pe_M) > 0 \tag{93}$$

and

$$\mu_1^{III} = \frac{1}{\frac{(Pe_M)^2}{4} + Pe_H\beta + a_3(Pe_H)}; \quad a_3(Pe_H) > 0 \tag{94}$$

Note in Equation (91) that $\hat{N}_1$, $\hat{N}_2$, and $\hat{N}_3$ are given by

$$\hat{N}_1 = \begin{cases} \sup_{0 \leq z \leq 1} \left[\exp\left(\frac{z}{2}(Pe_H - Pe_I)\right)\right] & \text{for } Pe_H > Pe_I \\ 1 \text{ for } Pe_H \leq Pe_I \end{cases} \tag{95}$$

and

$$\hat{N}_2 = \max\ (\hat{N}_{2,1}, \hat{N}_{2,3}) \tag{96}$$

$$\hat{N}_3 = \max\ (\hat{N}_{3,1}, \hat{N}_{3,2}) \tag{97}$$

where

$$\hat{N}_{2,1} = \begin{cases} \underset{0 \le z \le 1}{\text{Sup}} \left[\exp\left(\frac{z}{2} (Pe_I - Pe_M) \right) \right] \\ \qquad \text{for} \quad Pe_I > Pe_M \\ 1 \quad \text{for} \quad Pe_I \le Pe_M \end{cases} \tag{98}$$

$$\hat{N}_{2,3} = \begin{cases} \underset{0 \le z \le 1}{\text{Sup}} \left[\exp\left(\frac{z}{2} (Pe_H - Pe_M) \right) \right] \\ \qquad \text{for} \quad Pe_H > Pe_M \\ 1 \quad \text{for} \quad Pe_H \le Pe_M \end{cases} \tag{99}$$

and

$$\hat{N}_{3,1} = \begin{cases} \underset{0 \le z \le 1}{\text{Sup}} \left[\exp\left(\frac{z}{2} (Pe_I - Pe_H) \right) \right] \\ \qquad \text{for} \quad Pe_I > Pe_H \\ 1 \quad \text{for} \quad Pe_I \le Pe_H \end{cases} \tag{100}$$

$$\hat{N}_{3,2} = \begin{cases} \underset{0 \le z \le 1}{\text{Sup}} \left[\exp\left(\frac{z}{2} (Pe_M - Pe_H) \right) \right] \\ \qquad \text{for} \quad Pe_M > Pe_H \\ 1 \quad \text{for} \quad Pe_M \le Pe_H \end{cases} \tag{101}$$

If α_1 is such that the inequality

$$\alpha_1 < 1 \tag{102}$$

is satisfied, the operator $\hat{A}$ is a contraction mapping in $L_{2,3}$. Hence, applying the Contraction Mapping Theorem, the solution of Equation (66) is unique if Inequality (102) is satisfied.

Note that Inequality (102) is the uniqueness criterion for the temperature and concentration (initiator and monomer) profiles of the polyethylene TRAM. For a given solution of Equation (66) (that is, for given temperature and concentration profiles), if one wishes to show the uniqueness of the average molecular weight profile (number- and weight-average), one has to examine the uniqueness of the dead polymer moment profiles (that is, zeroth, first, and second moment), that is, of the solutions of Equations (52) for $i = 4$, 5, and 6. Now, it can be easily seen from Equations (53), (58), and (59) that the solutions of Equation (52) for $i = 5$ and 6 [that is, $\hat{y}_5(z)$ and $\hat{y}_6(z)$] will be unique if the solution of Equation (52) for $i = 4$ [that is, $\hat{y}_4(z)$] is unique.

The criterion for the existence and uniqueness of the steady state solution for Equation (52) for $i = 4$ may be derived in a manner similar to that shown above by developing a criterion for which the operation $\hat{A}_4$ is a contraction mapping in the function space $L_{2,1}[0, 1]$. This is done by first observing that [see Equation (42)]:

$$|f_4(z, y_4) - f_4(z, \psi)| \le N_{4,4} |y_4 - \psi_4| \tag{103}$$

where

$$N_{4,4} = \underset{\substack{0 \le z \le 1 \\ y_4 \in L_{2,1}}}{\text{Sup}} \left| \frac{\partial f_4}{\partial y_4} \right|$$

$$= \underset{0 \le z \le 1}{\text{Sup}} \left| \frac{Lk_{tr,P}}{v\nu^2} \{k_T + (C_4)_0 k_{tr,P}(1 - y_4(z))\} \right.$$

$$\left. \{2k_{tc}(Q_0^*)^2 + k_T Q_0^*\} - \left[\frac{L}{v} C_{M1^*}(z, y_4) k_{tr,P} \right] \right|$$

$$= \underset{0 \le z \le 1}{\text{Sup}} \left| \left[\frac{Lk_{tr,P}}{v\nu^2} \{k_T + (C_4)_0 k_{tr,P}\} \right. \right.$$

$$\left. \left. \{2k_{tc}(Q_0^*)^2 + k_T Q_0^*\} + \frac{L}{v} C_{M1^*}(z, y_4 = 1) k_{tr,P} \right] \right| \tag{104}$$

One can further show that $(\hat{A}_4 \hat{y}_4 - \hat{A}_4 \hat{\psi}_4)$ is bounded (Agrawal, 1974), that is,

$$||\hat{A}_4 \hat{y}_4 - \hat{A}_4 \hat{\psi}_4||^2_{L_{2,1}} \le (\alpha_2)^2 ||\hat{y}_4 - \hat{\psi}_4||^2_{L_{2,1}} \tag{105}$$

where α_2 is defined by

$$\alpha_2 = Pe_{M_r} N_{4,4} \mu_1^{IV} \tag{106}$$

Note that μ_1^{IV} is a function of Pe_{M_r} and is of the same form as Equation (93). If α_2 is such that the inequality

$$\alpha_2 < 1 \tag{107}$$

is satisfied, then the operator $\hat{A}_4$ is a contraction mapping in $L_{2,1}[0, 1]$. It then follows from the Contraction Mapping theorem that, for given temperature and concentration profiles, the solution of Equation (52) for $i = 4$ will exist and be unique if Inequality (107) is satisfied. Consequently, the average molecular weight (number- and weight-average) profiles will be unique if Inequalities (102) and (107) are satisfied.

Algorithms for Numerical Computation of Steady State Solution

It should be noted that the Contraction Mapping Theorem provides not only a uniqueness criterion for the solution of Equation (52) but also a numerical algorithm (successive approximation scheme) for obtaining the solution of the system Equation (52).

Hence if Inequality (102) is satisfied, the temperature and concentration profiles of the polyethylene TRAM can be computed from the algorithm given by

$$\hat{y}_i^{(n)} = \hat{A}_i \hat{y}_i^{(n-1)} \quad (i = 1, 2, 3) \tag{108}$$

[see Equations (66) to (68)]. Once the temperature and concentration profiles are computed by the above algorithm, profiles of the total dead polymer concentration can be computed by

$$\hat{y}_4^{(n)} = \hat{A}_4 \hat{y}_4^{(n-1)} \tag{109}$$

so long as Inequality (107) is satisfied. Note that Equations (108) and (109) may be rewritten more explicitly as

$$\hat{y}_1^{(n)}(z) = \int_0^1 \hat{k}_1(z, \xi) \hat{f}_1(\xi, y_1^{(n-1)}, y_3^{(n-1)}) \, d\xi \tag{110}$$

$$\hat{y}_2^{(n)}(z) = \int_0^1 \hat{k}_2(z, \xi) \hat{f}_2(\xi, y_1^{(n-1)}, y_2^{(n-1)}, y_3^{(n-1)}) \, d\xi \tag{111}$$

$$\hat{y}_3^{(n)}(z) = \int_0^1 \hat{k}_3(z, \xi) \hat{f}_3(\xi, y_1^{(n-1)}, y_2^{(n-1)}, y_3^{(n-1)}) \, d\xi \tag{112}$$

$$\hat{y}_4^{(n)}(z) = \int_0^1 \hat{k}_4(z, \xi) \hat{f}_4(\xi, y_4^{(n-1)}) \, d\xi \tag{113}$$

It should be noted that computation of the first and second moments of dead polymers [that is, solutions for $\hat{y}_5(z)$ and $\hat{y}_6(z)$] does not require an iterative method since they are easily computed by evaluating the follow-

TABLE 2. VALUES OF SYSTEM PARAMETERS

Initiator used:	T-Butyl hydroperoxide	Reactor diameter (D):	2.54 cm
Activation energy (E_d):	25,000 cal/g-mole*	Feed flow rate:	1.132×10^7 g/hr.
Reaction rate constant $(k_d)_0$	8.2×10^{11} (1/s)*	Heat capacity, C_p:	0.85 cal/g °C**
Reactor pressure (P)	2,500 atm.	Density of reactor fluid (ρ):	0.72 g/cm³**

* See Tobolsky (1954) and Guillet (1964).
** See American Petroleum Institute Data Book on Hydrocarbons (1968).

ing integrals:

$$\hat{y}_5(z) = \int_0^1 \hat{k}_5(z, \xi)\, \hat{f}_5(z, y_4)\, d\xi \qquad (114)$$

and

$$\hat{y}_6(z) = \int_0^1 \hat{k}_6(z, \xi)\, \hat{f}_6(z, y_4)\, d\xi \qquad (115)$$

RESULTS AND DISCUSSION

The successive approximation scheme given by Equations (110) to (112) is used for analysis of the effect of several important polyethylene reactor operating variables, such as initiator concentration, jacket temperature, etc., on monomer conversion and product properties (that is, molecular weight distributions). Since the numerical results were generated to gain some insight into the control and operation of the reactor, several simplifying assumptions were made as follows.

Polyethylene reactors are operated at high linear velocities (50 to 100 ft./s), and therefore the reactor pressure at the exit is lower than that at the entrance. Moreover, due to the increase in polymer concentration (hence an increase in viscosity), the pressure drop per unit length of the reactor will increase in the direction of the reactor exit. It is reported (Albright, 1974) that pressure drop in the reactor can range from 100 to 350 atm. Using published viscosity data on ethylene-polyethylene mixtures, we could compute the pressure drop and thus incorporate the effect of varying reactor pressure into the mathematical model. However, in order to simplify computation, it was assumed in the present study that reactor operating pressure is constant throughout the reactor. Since the polymerization rate is strongly dependent on pressure (see Table 1), the computed monomer conversions can be expected to be higher than encountered in commercial practice.

The calculations for conversion and product properties were made for a single injection of initiator along the tubular reactor. One reactor section consists of the preheating zone, reaction zone, and the cooling zone. Reaction sections are similar to each other from the standpoint of monomer conversion, but differ in the magnitude of long chain branching and, hence, in polydispersity. This is because, as will be seen below, long chain branching is dependent upon the polymer concentration.

The inside (wall) film resistance to heat transfer will be a function of the amount of polymer deposited on the walls of the reactor. Consequently, the overall heat transfer coefficient will vary along the length of the reactor and will be lower in the portions of the reactor where the temperatures are lower and the polymer concentrations higher. Since data on reactor heat transfer coefficient profiles is not available in the literature, it was assumed that the heat transfer coefficient is constant throughout the length of the reactor. Most of the computation was done by using an arbitrarily selected value of $U = 98.25$ cal/hr. cm² °C.

As mentioned above, polyethylene reactors are pulsed periodically, and this increases the degree of axial mixing. Although some data for the axial mixing diffusivity in tubes (as a function of Reynolds number) for steady flow are available in the literature (Levenspiel, 1962), there is no study reported in the literature which relates pulsing frequency and amplitude to axial mixing diffusivity. Therefore, in the present study the effect of axial mixing was investigated by varying the value of Peclet number.

The initiator and monomer concentration profiles, together with the reactor temperature profile, were computed by first selecting system parameters in such a way that Inequality (102) was satisfied. The computation was carried out using the iteration scheme given by Equations (110) to (112). The criteria used for convergence are

$$|\hat{y}_i^{(n)}(z) - \hat{y}_i^{(n-1)}(z)| \leq 0.005 \exp(-Pe\, z) \quad (i = 1, 2) \qquad (116)$$

and

$$|\hat{y}_3^{(n)}(z) - \hat{y}_3^{(n-1)}(z)| \leq 0.05 \exp(-Pe\, z) \qquad (117)$$

Note that when the solution is converged at the nth iteration, the error is given by

$$||\hat{\mathbf{Y}}^{(n)} - \hat{\mathbf{Y}}^*||_{L2,3} \leq \frac{(\alpha_1)^n}{1 - \alpha_1} ||\hat{\mathbf{Y}}^{(1)} - \hat{\mathbf{Y}}^{(0)}||_{L2,3} \qquad (118)$$

where α_1 is given by Inequality (102) and $\hat{\mathbf{Y}}^*$ is the solution sought for.

Table 2 gives numerical values of the system parameters (for example, reaction rate constant, activation energy, etc.) used for obtaining the results presented. It should be mentioned that the values of system parameters were taken from the literature wherever possible and that some reasonable guesses had to be made by exercising our understanding of the industrial practice in operating high pressure polyethylene tubular reactors. The diameter of the reactor was assumed to be 2.54 cm. Two different reactor lengths were investigated, namely, 457 and 1525 m. It is reported (Albright, 1974) that reactor diameters are in the range of 25 to 76 mm, and that reactor lengths vary from 245 to 760 m. The feed flow rate was chosen to be 1.132×10^7 g/hr. This gives a reactor residence time of 50 s for the case of $L = 457$ m, and a residence time of 165 s for the case of $L = 1525$ m. It is reported (Albright, 1974) that reactor residence times vary from 45 to 60 s. The references for the ethylene transport properties (density and heat capacity) and the initiator properties (rate constant, activation energy) used in the computation are given in Table 2.

It should be noted that we assumed chain transfer reactions to monomer and initiator to be negligible, that the initiator efficiency is independent of pressure, and that the intramolecular chain transfer reaction, which gives rise to short chain branching, is not important (relative to molecular weight distribution) compared to the intermolecular chain transfer reaction, which gives rise to long chain branching.

Effect of Heat Transfer on Reactor Performance

From the standpoint of heat transfer, the reactor can be viewed as consisting of two zones. In the first zone (the

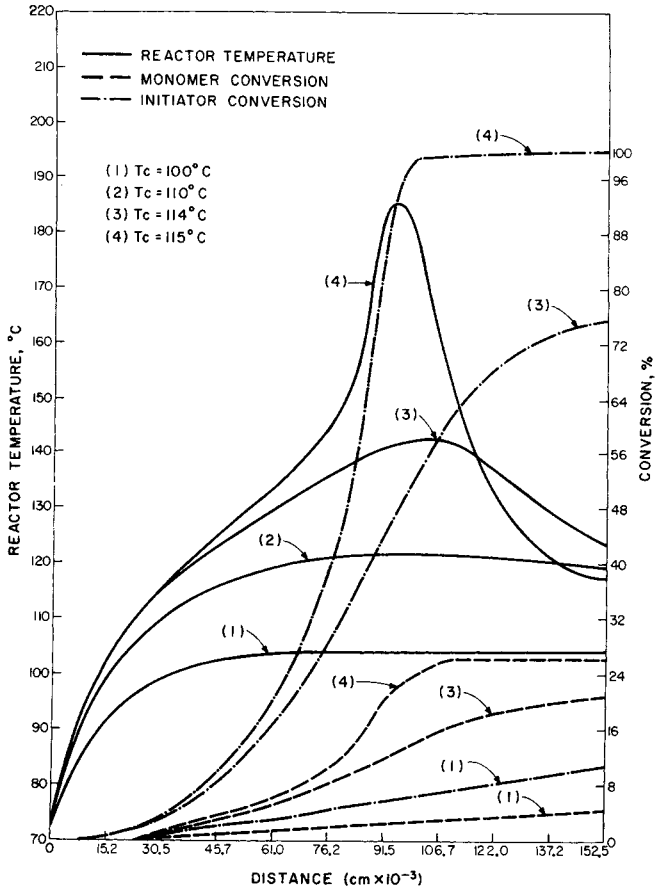

Fig. 1. Reactor temperature and concentration profiles as a function of jacket fluid temperature for $U = 98.25$ cal/hr. cm^2 °C, $Pe = 100$, $T_0 = 70$°C and $(C_I)_0 = 8.3 \times 10^{-7}$ g-moles/cc.

so-called "preheating zone"), the feed is raised to initiation temperature by external heating, and in the second zone (the so-called "cooling zone"), the heat of reaction is removed by external cooling. As indicated earlier, both the heating of the feed and the removal of the reaction heat can be accomplished with a constant jacket fluid temperature, or with a combination of a high jacket temperature for preheating and a low jacket temperature for removing the heat of reaction. It should be noted that the actual value of the jacket temperature used is also governed by the degree of polymer plating on the wall of the reactor since lower jacket temperatures would increase the polymer build-up and hence adversely affect the heat transfer coefficient. Since data on jacket temperatures are not available in the literature, values of jacket temperature were selected to give a reasonable monomer conversion.

Let us first consider the case where the jacket temperature is kept constant throughout the entire reactor. The temperature and concentration profiles are given in Figures 1 and 2 for $U = 98.25$ and 196.5 cal/hr. cm^2 °C, respectively.

It is seen in Figure 1 that the reactor with $U = 98.25$ cal/hr. cm^2 °C requires a longer preheating zone, as reflected by the longer distance from the inlet at which a peak temperature occurs, compared to that for $U = 196.5$ cal/hr. cm^2 °C shown in Figure 2. Although an increase in jacket temperature reduces the distance at which a peak temperature occurs and requires a shorter reactor length for preheating the feed to initiation temperature, the system becomes sensitive to variations in jacket temperature. For example, it can be seen from Figure 1 that an increase in jacket temperature from 114° to 115°C increases the peak temperature by 40°C. At higher jacket temperatures, one would expect to have greater sensitivity. Consequently, stable reactor operation requires a low jacket temperature which, in turn, requires a longer reactor. Note in Figure 1, however, that an increase in jacket temperature also brings about a higher reactor temperature, which results in an increase in initiator and monomer conversion.

For the reactor system with a higher heat transfer coefficient, higher jacket temperatures are permissible while keeping the reactor less sensitive to the variations in jacket temperature (see Figure 2). This results in a shorter preheating zone. Thus, for the same range in monomer conversion (4.50% to 24%), the distance at which a peak temperature occurs, for the system with $U = 196.5$ cal/hr. cm^2 °C, is in the range of 6.87×10^4 to 3.80×10^4 cm. Hence, for the same monomer conversion, a system with a higher heat transfer coefficient should require a shorter reactor. For example, it may be seen in Figure 2 that, for $U = 196.5$ cal/hr cm^2 °C, if we select a jacket temperature of 120°C, a monomer conversion of 13% can be obtained in a reactor length of only 9.95×10^4 cm. Note that, for such a reactor, a change in the jacket temperature of 5°C increases the peak temperature by only 9°C. On the other hand, for the system with $U = 98.25$ cal/hr cm^2 °C, the same monomer conversion requires a jacket temperature of at least 110°C and a reactor length of 15.25×10^4 cm. Therefore in this case not only must the reactor be longer, but it is also more sensitive to variation in jacket temperature. Note that a change in jacket temperature of 5°C increases the peak temperature by 61°C. This indicates also that reactor fouling can affect the stability of the reactor significantly.

The temperature and concentration profiles for different

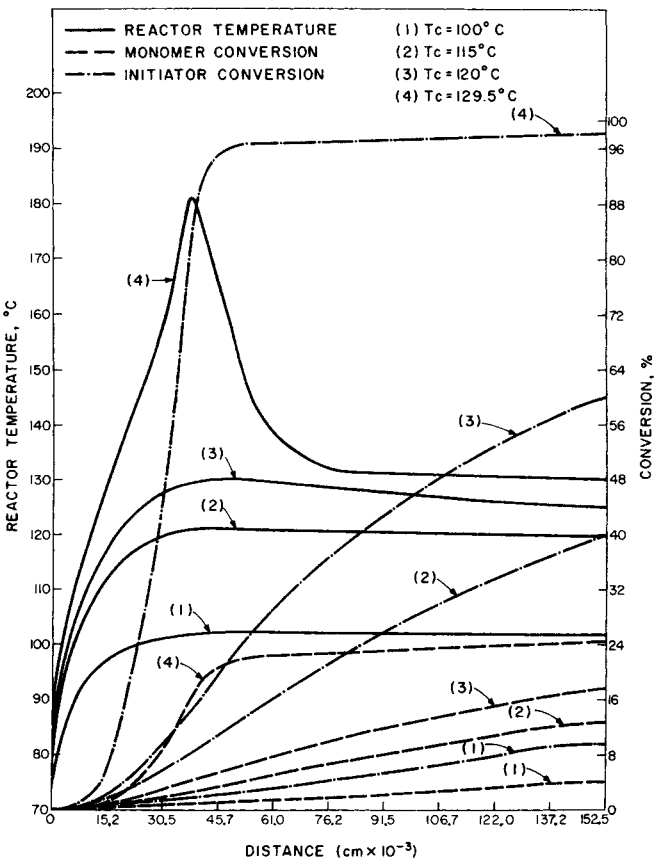

Fig. 2. Reactor temperature and concentration profiles as a function of jacket fluid temperature for $U = 196.5$ cal/hr. cm^2 °C, $Pe = 100$, $T_0 = 70$°C and $(C_I)_0 = 8.3 \times 10^{-7}$ g-moles/cc.

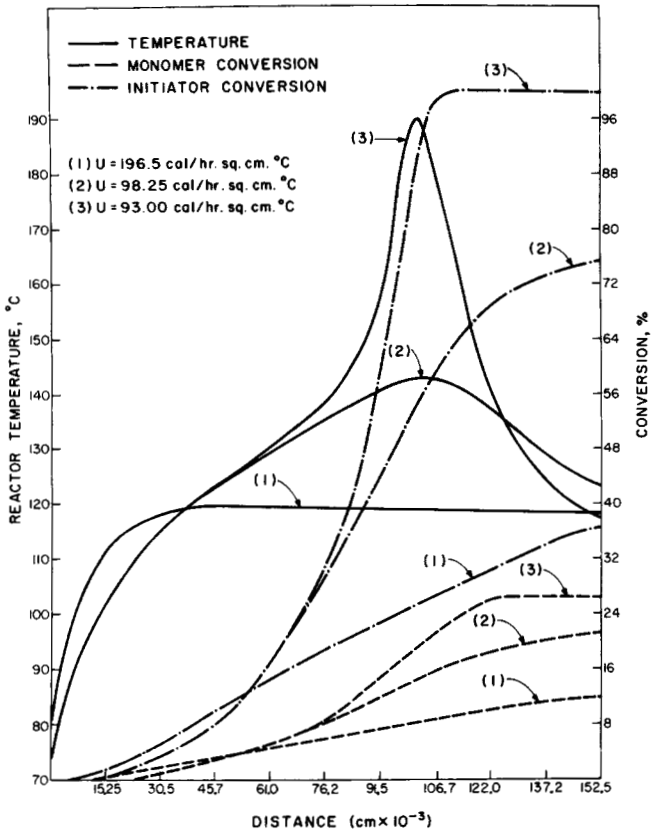

Fig. 3. Reactor temperature and concentration profiles as a function of heat transfer coefficient for $T_c = 114°C$, $Pe = 100$, $T_0 = 70°C$ and $(C_I)_0 = 8.3 \times 10^{-7}$ g-moles/cc.

values of the heat transfer coefficient are given in Figure 3. As the heat transfer coefficient is reduced, both the peak reactor temperature and the distance for peak temperature increase. In spite of the increase in the distance for peak temperature, reactor temperatures in the cooling zone are higher (see Figure 3) and hence both initiator and monomer conversions increase with a decrease in heat transfer coefficient. Note that, for the case where $U = 0$ (adiabatic reactor), the initiator and monomer conversion are negligible. This is due to the fact that the feed cannot be preheated to initiation temperatures.

Let us now consider the case for which different jacket temperatures are used in the preheating and cooling zones of the reactor. The temperature and concentration profiles are given in Figure 4. Note that the jacket temperature in the cooling zone of the reactor, $0 \leq L \leq 1.78 \times 10^4$, is kept constant at 50°C. Note further that in Figure 4 the computations were carried out for a reactor length of 4.57×10^4 cm. With a higher jacket temperature in the preheating zone, a shorter reactor is required to preheat the feed up to initiation temperatures, as may be seen in Figure 4. It is seen that, for a monomer conversion in the range of 5.0% to 13.0%, the distance for peak temperature lies somewhere in the range of 2.06×10^4 cm to 1.83×10^4 cm, as opposed to a range of 10.7×10^4 cm to 9.95×10^4 cm for the reactor with a fixed jacket temperature for the entire reactor (see Figure 4).

Effect of Feed Conditions on Reactor Performance

The temperature and concentration profiles for different values of the feed initiator concentration are given in Figure 5 and in Figure 6 for different values of the feed tem-

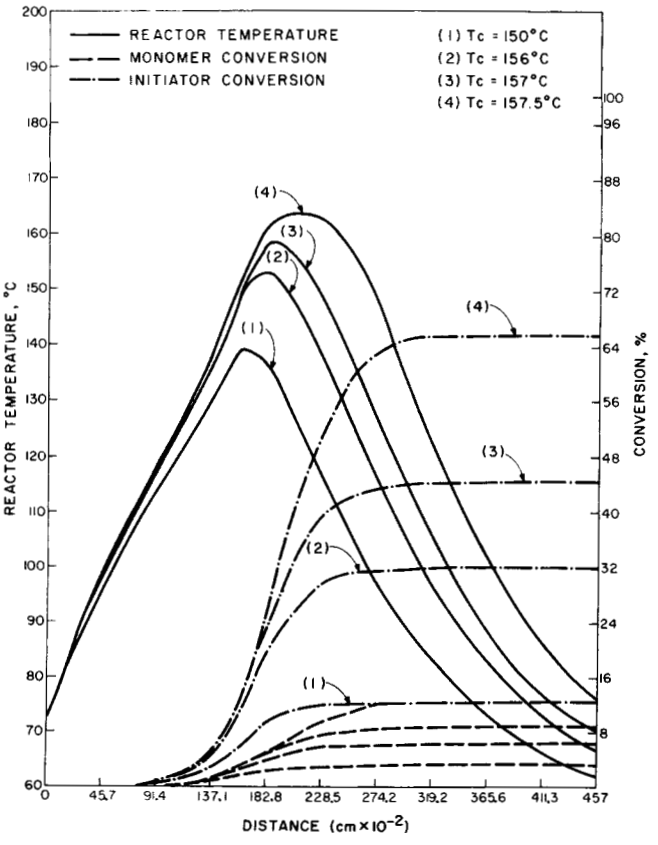

Fig. 4. Reactor temperature and concentration profiles as a function of preheating zone jacket temperature for $U = 98.25$ cal/hr. cm² °C, $Pe = 100$, $T_0 = 70°C$, and $(C_I)_0 = 8.3 \times 10^{-7}$ g-moles/cc.

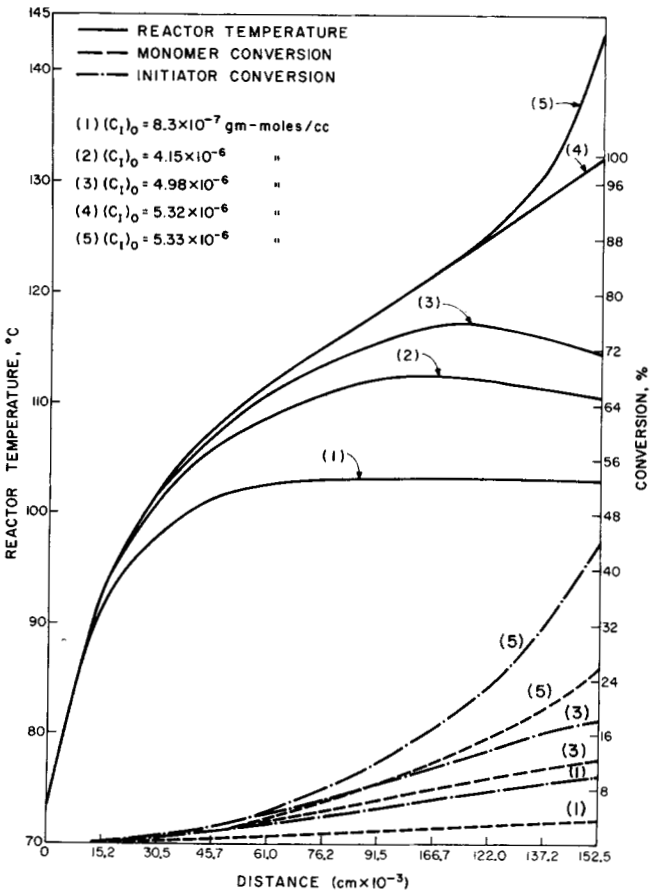

Fig. 5. Reactor temperature and concentration profiles as a function of feed initiator concentration for $U = 98.25$ cal/hr. cm² °C, $Pe = 100$, $T_0 = 70°C$, and $T_c = 100°C$.

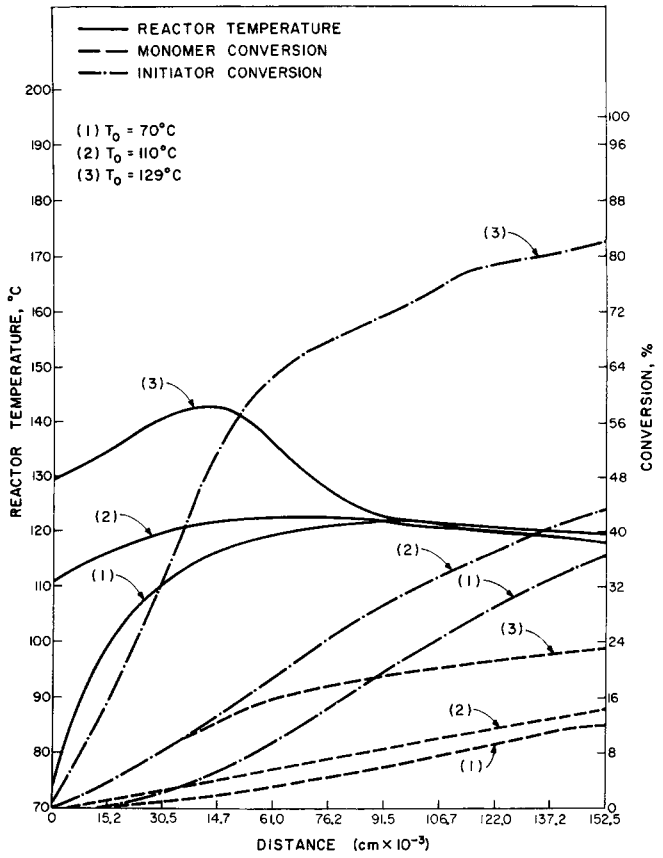

Fig. 6. Reactor temperature and concentration profiles as a function of feed temperature for $U = 98.25$ cal/hr. cm^2 °C, $Pe = 100$, $T_c = 110$°C and $(C_I)_0 = 8.3 \times 10^{-7}$ g-moles/cc.

perature. Since the polymerization rate is proportional to the square root of the initiator concentration, as the initiator concentration is increased the monomer conversion is increased accordingly. As a consequence, both the peak temperature and initiator conversion also increase. Thus, an increase in initiator concentration brings about a high monomer conversion even at a low jacket temperature. For example, at a jacket temperature of 100°C, one can increase monomer conversion from 3.65% to 25.5% by increasing the initiator concentration from 8.3×10^{-7} to 5.33×10^{-6} g-moles/cc. However, this also brings about an increased sensitivity to perturbations in feed concentration. An increase of 7% in the initiator concentration from 4.98×10^{-6} to 5.33×10^{-6} g-moles/cc increases the peak temperature by 27°C. Note that an increase in feed concentration also increases the distance for peak temperatures. For an initiator concentration greater than 5.15×10^{-6} g-moles/cc, the heat generation rate of the reactor exceeds the heat removal rate at all points. Consequently, the peak temperature occurs at the end of the reactor. A further increase in feed initiator concentration increases the peak temperature at an explosive rate. For example, an increase of initiator concentration by 0.2% (from 5.32×10^{-6} to 5.33×10^{-6} g-moles/cc) increases the peak temperature by 11°C.

With an increase in reactor feed temperature T_0, the distance for peak temperature decreases. This is as expected because a shorter reactor is required to heat the feed to initiation temperature. Thus, an increase in the feed temperature from 70° to 120°C reduces the distance for peak temperature from 9.94×10^4 to 4.57×10^4 cm. Varying the feed temperature from 70° to 100°C leaves the peak temperature unchanged. For $T_0 > 100$°C, the reactor peak temperature increases at an increasing rate. It can also be seen from Figure 6 that an increase in T_0 increases the reactor temperature, and hence the initiator and monomer conversion, to be higher in the preheating zone of the reactor. Consequently initiator and monomer conversion will increase with an increase in feed temperature.

Effect of Axial Mixing on Reactor Performance

The effect of mixing on conversion and peak temperature was studied by varying the Peclet number. The temperature and concentration profiles are given in Figure 7. It is seen in Figure 7 that, as the degree of axial mixing in the reactor is increased (that is, as the Peclet number is reduced), the temperature and concentration profiles in the reactor flatten. Thus a decrease in the Peclet number brings about a higher reactor temperature and higher conversion of initiator and monomer in the preheating zone, whereas it brings about a lower peak temperature and lower overall conversion at the reactor exit. Since commercial reactors are pulsed periodically, one may expect the monomer conversion to decrease with an increase in the frequency (or severity) of pulsing.

Number-Average Molecular Weight and Polydispersity without Chain Transfer Reactions

The number- and weight-average molecular weights were computed by first solving Equation (52) for $i = 4$ for the total dead polymer concentration (the zeroth moment of dead polymer). This was done by using the successive approximation scheme given by Equation (113), together with the temperature and concentration (initiator and monomer) profiles computed first. Once the zeroth moment of the total dead polymer is computed, the first

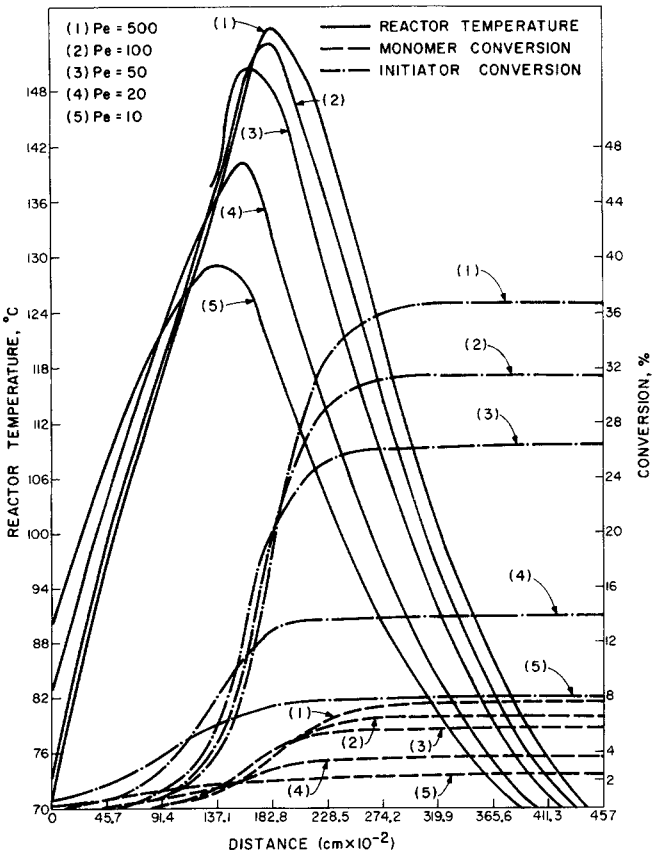

Fig. 7. Reactor temperature and concentration profiles as a function of Peclet number for $U = 98.25$ cal/hr. cm^2 °C, $T_0 = 70$°C, $T_{c1} = 156$°C, $T_{c2} = 50$°C and $(C_I)_0 = 8.3 \times 10^{-7}$ g-moles/cc.

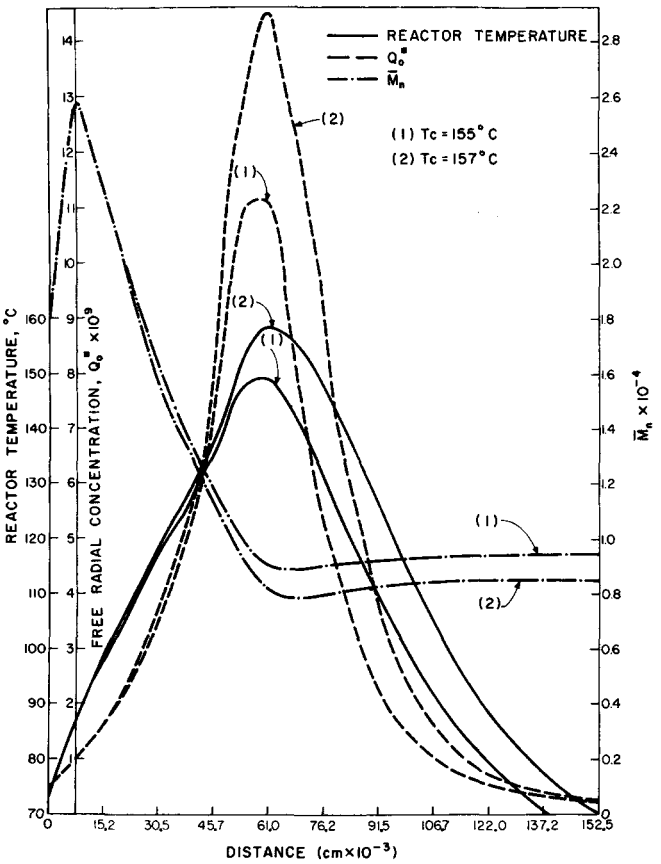

Fig. 8. Reactor temperature, free-radical concentration, and number-average molecular weight profiles for $U = 98.25$ cal/hr. cm² °C, $T_{c2} = 50$°C, $Pe = 100$, $T_0 = 70$°C, and $(C_I)_0 = 8.3 \times 10^{-7}$ g-moles/cc.

and second moments of dead polymer are found by solving Equations (114) and (115), respectively, and then the number- and weight-average molecular weight are computed by using Equations (28) and (29), respectively. The average molecular weights were computed by both including and excluding chain transfer reactions from the reaction kinetics. Let us first consider the case for which chain transfer reaction rates are negligible.

Profiles of the reactor temperature, the total free radical concentration Q_0^* and the number-average molecular weight $\overline{M}_n$ are given in Figure 8. It is seen in Figure 8 that changes in both the free radical concentration and the number-average molecular weight are closely related to the changes in reactor temperature. Thus, as the reactor temperature increases, Q_0^* also increases, while $\overline{M}_n$ decreases. Conversely, as the reactor temperature decreases, Q_0^* also decreases while $\overline{M}_n$ increases slightly.

Now, note that the total free radical termination rate, or the rate at which dead polymer chains are being formed, is given by

$$R_{tc,M_r} = k_{tc}(Q_0^*)^2 \qquad (119)$$

and the overall polymerization rate is given by

$$R_p = k_p C_M Q_0^* \qquad (120)$$

Since the increase in the propagation rate k_p with temperature is less than that in Q_0^*, the increase in the total free radical termination rate is greater than that in the overall polymerization rate. Hence, as the reactor temperature rises, the number-average molecular weight of the dead polymer being formed is reduced. Similarly, since the decrease in R_{tc,M_r} is greater than that in R_p, as the reactor temperature decreases, the number-average molecular weight of the dead polymer being formed will increase. Note further in Figure 8 that although the reactor temperature is reduced significantly in the cooling zone of the reactor, the increase in M_n is relatively small. This is attributable to the fact that very little monomer conversion takes place in this portion of the reactor. (See Figure 4).

On the basis of the above discussion, it can be seen that the temperature profile in the reactor has a strong influence on the number-average molecular weight of the product $\overline{M}_n$. Since, as discussed above, the reactor temperature profile is affected by various operating variables, one can expect $\overline{M}_n$ to vary with the jacket temperature, initiator concentration, etc. The number-average molecular weight $\overline{M}_n$, and polydispersity $\overline{M}_w/\overline{M}_n$, which is defined as the ratio of weight- to number-average molecular weight, are listed in Table 3 for various values of feed temperature, jacket temperature, initiator concentration, and the Peclet number.

If we take a close look at Table 3, it can be seen that $\overline{M}_n$ decreases rapidly as the feed initiator concentration is increased. This is attributable to the fact that, with an increase in initiator concentration, the free radical concentration Q_0^* increases the reactor temperature, which in turn increases the rate of termination of the polymerization reaction. For instance, increasing the initiator concentration from 8.3×10^{-7} to 5.33×10^{-6} g-moles/cc causes a decrease in $\overline{M}_n$ from 640,000 to 156,000.

TABLE 3. EFFECT OF REACTOR OPERATING CONDITIONS ON THE NUMBER-AVERAGE MOLECULAR WEIGHT ($\overline{M}_n$) AND POLYDISPERSITY ($\overline{M}_w/\overline{M}_n$)

Reactor variables	Number-average molecular weight ($\overline{M}_n$)	Polydispersity ($\overline{M}_w/\overline{M}_n$)
A. Jacket temperature, °C		
100	522,000	1.5
110	398,000	1.5
113	348,000	1.5
114	333,000	1.5
115	312,000	1.5
B. Initiator concentration, g-moles/cc		
8.3×10^{-7}	640,000	1.5
1.66×10^{-6}	432,000	1.5
3.32×10^{-6}	272,000	1.5
4.98×10^{-6}	200,000	1.5
5.32×10^{-6}	165,000	1.5
5.33×10^{-6}	156,000	1.5
C. Feed temperature, °C		
70	398,000	1.5
120	372,000	1.5
122	368,000	1.5
128	340,000	1.5
128.5	336,000	1.5
129.0	333,000	1.5
D. Peclet number		
500	246,000	1.5
100	253,000	1.5
50	262,000	1.5
20	308,000	1.5
10	362,000	1.5

The effect of axial mixing on $\overline{M}_n$ was also studied by varying the Peclet number. It can be seen from Table 3 that as the Peclet number is decreased, $\overline{M}_n$ is increased. For instance, as the Peclet number is reduced from 500 to 10, $\overline{M}_n$ increases from 246,000 to 362,000. It can be then concluded that pulsing the reactor fluid will affect not only the monomer conversion, but also the number-average molecular weight.

On examining Table 3, it is seen that the polydispersity is not affected by variations in reactor variables, giving a constant value of $\overline{M}_w/\overline{M}_n = 1.5$. This is due to the absence of any chain transfer reactions.

Effect of Chain Transfer to Dead Polymer on Molecular Parameters

Polyethylene made by the high pressure process is characterized by a high value of polydispersity. This is attributed to the occurrence of chain transfer from free radicals to dead polymer chains, giving rise to long chain branching. Let us then examine the effects of varying long chain branching reaction rates on the molecular weight and its distribution. Note that the effect of long chain branching was investigated for the case where there is no chain transfer reaction in monomer and modifier is absent.

The zeroth (Q_0), first (Q_1) and second (Q_2) moments of dead polymer, together with the number-average molecular weight and polydispersity, are given in Table 4 as functions of the ratio of the long chain branching reaction rate constant to the propagation rate constant at a low reaction temperature. Now, it is seen in Table 4 that, as the long chain branching reaction rate constant is increased, there is no significant change in Q_0 and Q_1, but the increase in Q_2 is pronounced. Consequently, whereas the number-average molecular weight is unchanged, a pronounced increase in polydispersity is seen as $k_{tr,P}/k_P$ increases.

It should be remembered that every occurrence of chain transfer to dead polymer leaves the total number of dead polymer chains unchanged, except for the case of chain transfer from a monomer free radical, that is, M_1^*. Therefore, so long as the chain transfer from a monomer free radical is negligible, that is, when $k_{tr,P}\, Q_0\, C_{M1^*} << k_{tc}(Q_0^*)^2$ in the rate equation for total dead polymer [see Equation (4)], the total dead polymer concentration will not be affected by changes in long chain branching reaction rates. If we examine the rate equation for the first moment of dead polymer [see Equation (36)] it can be seen that $k_{tr,P}\, Q_0\, C_{M1^*} << k_P\, C_M\, Q_0^*$, and hence Q_1, does not vary with changes in long chain branching reaction rates. Hence, so long as the chain transfer from a monomer free radical is negligible, the number-average molecular weight will not vary with changes in long chain branching reaction rates. We will show later that there are conditions under which the chain transfer rate from monomer free radicals (M_1^*) to dead polymers is not negligible and, in such situations, the number-average molecular weight will vary significantly with changes in long chain branching reaction rate.

We have seen above that, when chain transfer reactions do not occur, the polydispersity is unaffected. We have also seen that, although the number-average molecular weight varies because of the change in free radical concentration that occurs with long chain branching, the polydispersity also varies with changes in Q_0^*, the total number of free radicals. This is because an increase in Q_0^* increases the overall long chain branching rate, which in turn increases the second moment of dead polymer, Q_2^*. Note from Equations (4) and (36) that increasing Q_0^* will bring about an increase in the zeroth and first moments of dead polymer. As a result, although both the number- and weight-average molecular weight decrease, the polydispersity increases because $\overline{M}_n$ decreases more than M_w does. This may be seen in Table 5, in which the polymer moments, together with $\overline{M}_n$ and polydispersity, are given as functions of the free-radical concentration for a fixed

Table 4. Effect of Varying Long Chain Branching Rate on Average Molecular Weight and Its Distribution at a Low Reactor Temperature

$k_{tr,p}/k_p$ at 70°C	Q_0 $\left(\frac{\text{g-moles}}{\text{cc}}\right)$	Q_1 $\left(\frac{\text{g-moles}}{\text{cc}}\right)$	Q_2 $\left(\frac{\text{g-moles}}{\text{cc}}\right)$	$\overline{M}_n$	$\overline{M}_w/\overline{M}_n$
0.000	0.5060×10^{-6}	0.6×10^{-2}	1.07×10^{2}	333,000	1.50
0.065	0.5060×10^{-6}	0.6×10^{-2}	1.155×10^{2}	333,000	1.62
0.325	0.5060×10^{-6}	0.6×10^{-2}	1.32×10^{2}	333,000	1.85
0.650	0.5060×10^{-6}	0.6×10^{-2}	1.50×10^{2}	333,000	2.10
6.500	0.5060×10^{-6}	0.6×10^{-2}	0.2295×10^{3}	333,000	3.20

System parameters: $Pe = 100$, $L = 15.25 \times 10^4$ cm, $T_0 = 70$°C, $T_c = 114$°C, $U = 98.25$ cal/hr cm² °C.

Table 5. Effect of Varying Free Radical Concentration on Average-Molecular Weight and Its Distribution

Q_0^* $\left(\frac{\text{g-moles}}{\text{cc}}\right)$	Q_0 $\left(\frac{\text{g-moles}}{\text{cc}}\right)$	Q_1 $\left(\frac{\text{g-moles}}{\text{cc}}\right)$	Q_2 $\left(\frac{\text{g-moles}}{\text{cc}}\right)$	$\overline{M}_n$	$\overline{M}_w/\overline{M}_n$
		$k_{tr,p}/k_p = 0.65$ at 70°C			
0.390×10^{-10}	0.514×10^{-6}	0.602×10^{-2}	0.150×10^{3}	333,000	2.1
0.387×10^{-9}	0.506×10^{-4}	0.609×10^{-1}	0.232×10^{3}	33,800	3.2
0.756×10^{-9}	0.195×10^{-3}	0.122×10^{0}	0.262×10^{3}	17,500	3.4
0.314×10^{-8}	0.186×10^{-2}	0.494×10^{0}	0.460×10^{3}	7,400	3.6

System parameters: $Pe = 100$, $L = 15.25 \times 10^4$ cm, $T_0 = 70$°C, $T_c = 114$°C, $U = 98.25$ cal/hr. cm² °C, $(Cr)_0 = 8.3 \times 10^{-7}$ g-moles/cc.

Table 6. Effect of Varying Long Chain Branching Rate on Average Molecular Weight and Its Distribution at a High Reactor Temperature

$k_{tr,p}/k_p$ at 70°C	Q_0 $\left(\frac{\text{g-moles}}{\text{cc}}\right)$	Q_1 $\left(\frac{\text{g-moles}}{\text{cc}}\right)$	Q_2 $\left(\frac{\text{g-moles}}{\text{cc}}\right)$	$\overline{M}_n$	$\overline{M}_w/\overline{M}_n$
0.0000	0.173×10^{-2}	0.250×10^{-1}	0.740×10^{4}	40,000	1.50
0.0650	0.126×10^{-2}	0.250×10^{-1}	0.182×10^{5}	55,500	3.70
0.3250	0.520×10^{-3}	0.250×10^{-1}	0.515×10^{5}	135,000	4.30
0.6500	0.284×10^{-3}	0.250×10^{-1}	0.128×10^{6}	246,000	5.80
0.9900	0.188×10^{-3}	0.250×10^{-1}	0.253×10^{6}	372,000	7.80
1.7000	0.111×10^{-3}	0.250×10^{-1}	0.732×10^{6}	630,000	13.00

Reactor Conditions: Initiator and monomer concentration profile was as in Figure 1 for T_c = 114°C. Temperature at every point in the reactor was greater by 90°C as compared to the temperature profile in Figure 1 for T_c = 114°C.

Table 7. Effect of Using Modifiers on Average Molecular Weight and Its Distribution

Mole ratio of modifier to monomer	Q_0 $\left(\frac{\text{g-moles}}{\text{cc}}\right)$	Q_1 $\left(\frac{\text{g-moles}}{\text{cc}}\right)$	Q_2 $\left(\frac{\text{g-moles}}{\text{cc}}\right)$	$\overline{M}_n$	$\overline{M}_w/\overline{M}_n$
		$k_{tr,p}/k_p = 0.325$ at 70°C			
0.00	0.506×10^{-6}	0.604×10^{-2}	0.116×10^{3}	333,000	1.6
0.01	0.966×10^{-6}	0.604×10^{-2}	0.790×10^{2}	174,000	2.1
0.05	0.272×10^{-5}	0.604×10^{-2}	0.317×10^{2}	62,000	2.4
0.10	0.470×10^{-5}	0.604×10^{-2}	0.190×10^{2}	35,800	2.5
		$k_{tr,p}/k_p = 6.5$ at 70°C			
0.00	0.506×10^{-6}	0.604×10^{-2}	0.230×10^{3}	333,000	3.2
0.01	0.966×10^{-6}	0.604×10^{-2}	0.118×10^{3}	181,000	3.1
0.05	0.275×10^{-5}	0.604×10^{-2}	0.413×10^{2}	62,000	3.0
0.10	0.465×10^{-3}	0.604×10^{-2}	0.238×10^{2}	36,100	3.0

System parameters: Pe = 100, $L = 15.25 \times 10^4$ m, T_0 = 70°C, T_c = 114°C, U = 98.25 cal/hr. cm² °C, $(Ct)_0 = 8.3 \times 10^{-7}$ g-moles/cc.

value of $k_{tr,P}/k_P = 0.65$. For example, increasing Q_0^* by a factor of 80 decreases $\overline{M}_n$ from 333,000 to 7,400, and increases polydispersity from 2.1 to 3.6.

We have discussed above the effect of the ratio of the long chain branching reaction rate constant to the propagation rate constant on the molecular weight and its distribution. It is interesting to note that a higher reactor temperature will increase not only the long chain branching rates (at a fixed value of $k_{tr,P}/k_P$), but also the concentration of free radicals. This is attributable to the higher initiator decomposition rates. Table 6 gives some representative results for a higher reactor temperature.

It is seen in Table 6 that, as the value of $k_{tr,P}/k_P$ is increased beyond 0.0065, the total dead polymer concentration begins to drop significantly. This is because, at higher reactor temperatures, the chain transfer from the monomer free radical to dead polymer becomes significant. That is, the magnitude of the term $k_{tr,P} Q_0 C_{M1^*}$ in Equation (4) is comparable to the term $k_{tc}(Q_0^*)^2$ for values of $k_{tr,P}/k_P > 0.0065$.

Since the chain transfer from the monomer free radical brings about a decrease in the number of dead polymer chains, the polymer concentration drops. In addition, it can be seen that the value of Q_2 increases rapidly. If we compare the data in Tables 4 and 6, it can be seen that increasing $k_{tr,P}/k_P$ from 0 to 6.5 at low temperatures does not affect $\overline{M}_n$, but increases polydispersity from 1.5 to 3.2, whereas increasing $k_{tr,P}/k_P$ from 0 to 1.7 at high temperatures increases $\overline{M}_n$ from 40,000 to 630,000 and also increases polydispersity from 1.5 to 13.0.

Reactor conditions, similar to those discussed above, can be obtained, for example, by using a high temperature initiator, that is, by using an initiator with high values of $(k_d)_0$ (specific reaction rate constant) and high activation energy. Use of such an initiator will require higher reactor temperatures in order to obtain the same degree of conversion.

It may be seen from the above discussion that a selection of different types of initiator (for example, low, medium, or high temperature) will also affect both the average molecular weight ($\overline{M}_n$ and M_w) and its distribution. In industrial practice, a proper combination of low, medium, and high temperature initiators is used to achieve the desired molecular weight and its distribution.

Effect of Chain Transfer to Modifier on Molecular Parameters

Commercial polyethylene producers also use modifiers (or solvents) to regulate the molecular weight and its distribution. The effects on the polymer moments and polydispersity of varying the modifier concentration were investigated for two different levels of long chain branching, that is, two different values of $k_{tr,P}/k_P$, as given in Table 7. The computations were made by selecting propane as the modifier. Note that in order to compute the polymer moments in the presence of modifiers it was first necessary to solve the system equations for the modifier concentration profile in the reactor. This was done by applying the successive iteration scheme.

If we examine the rate equation for dead polymer concentration [see Equation (4)], it can be seen that increasing the modifier concentration will increase the number of dead polymer chains. It can also be seen, from Equations (36) and (37) that, for $k_T << k_P C_M$, Q_1 will not be affected by an increase in modifier concentration, whereas Q_2 will decrease, and $\overline{M}_n$ will decrease. This is seen in Table 7. For example, for $k_{tr,P}/k_P = 0.325$ increasing the modifier concentration by a factor of ten decreases $\overline{M}_n$ from 333,000 to 35,800, and increases the polydispersity from 1.6 to 2.5. It is interesting to note that, at much higher values of $k_{tr,P}/k_P$, the polydispersity decreases slightly.

ACKNOWLEDGMENT

This work is partly taken from the dissertation of S. Agrawal, submitted to the Faculty of the Polytechnic Institute of New York in partial fulfillment of requirements for the degree of doctor of philosophy, 1974.

NOTATION

$\hat{\mathbf{A}}$ = integral operator (vector) defined in Equation (66)

$B_1 = \left\{ \frac{(-\Delta H)_d (C_I)_0}{\rho C_p T_0} \right\} \left\{ \frac{\hat{E}_d}{RT_0} \right\}$

$B_2 = \left\{ \frac{(-\Delta H)_p (C_M)_0}{\rho C_p T_0} \right\} \left\{ \frac{\hat{E}_d}{RT_0} \right\}$

C_I = concentration of initiator in the reactor, moles/unit volume

$(C_I)_0$ = concentration of initiator in feed stream, moles/unit volume

C_M = concentration of monomer, moles/unit volume

$(C_M)_0$ = concentration of monomer in feed stream, moles/unit volume

C_{M_r} = concentration of the dead polymer of chain length r, moles/unit volume

$(C_{M_r})_0$ = concentration of dead polymer M_r in feed stream, mole/unit volume

$C_{M_1^*}$ = concentration of an active monomer, moles/unit volume

$C_{M_r^*}$ = concentration of the active polymer of chain length r, moles/unit volume

$(C_4)_0$ defined as $\sum_{r=2}^{\infty} (C_{M_r})_0$, moles/unit volume

$(C_5)_0$ defined as $\sum_{r=2}^{\infty} (r\, C_{M_r})_0$, moles/unit volume

$(C_6)_0$ defined as $\sum_{r=2}^{\infty} (r^2\, C_{M_r})_0$, moles/unit volume

C_S = concentration of modifier, moles/unit volume

C_P = specific heat of the feed and of effluent stream

D = tube diameter

Da_I = Dahmkohler number for initiator defined as $L(k_d)_0 \exp(-\hat{E}_d/RT_0)/v$

Da_M = Dahmkohler number for monomer defined as $\left\{ \frac{L^2}{v^2} \frac{(k_P)_0^2 (k_{d\epsilon})_0 (C_I)_0}{(k_{tc})_0} \exp(-\hat{E}_{pol}/RT_0) \right\}^{1/2}$

$\hat{D}_I$ = axial mass diffusivity for initiator

$\hat{D}_M$ = axial mass diffusivity for monomer

$\hat{D}_{M_r}$ = axial mass diffusivity for dead polymer of chain length r

$\hat{E}_d$ = activation energy for decomposition reaction

$\hat{E}_i$ = activation energy for chain initiation reaction

$\hat{E}_p$ = activation energy for propagation reaction

$\hat{E}_{pol}$ = activation energy for chain polymerization

$\hat{E}_{tc}$ = activation energy for chain termination by recombination

$\hat{E}_{tr,P}$ = activation energy for chain transfer to dead polymer

$\hat{E}_{tr,M}$ = activation energy for chain transfer to monomer

$\hat{E}_{tr,S}$ = activation energy for chain transfer to modifier

$(-\Delta H)_d$ = heat of initiator decomposition reaction

$(-\Delta H)_p$ = heat of chain propagation reaction

I = initiator

k_d = reaction rate constant for initiator decomposition

k_p = reaction rate constant for chain propagation

k_{tc} = reaction rate constant for chain termination by recombination

k_{td} = reaction rate constant for chain termination by disproportionation

$k_{tr,P}$ = reaction rate constant for chain transfer to polymer

$k_{tr,M}$ = reaction rate constant for chain transfer to monomer

$k_{tr,S}$ = reaction rate constant for chain transfer to modifier

k_T as defined by Equation (6)

$\hat{K}_L$ = axial thermal diffusivity

L = length of reactor

$L_{2,N}[0, 1]$ = square-integrable function space defined as the set of N vector-valued measurable function in the interval [0, 1]

M = monomer molecule (C_2H_4)

M_1^* = monomer free radical

$\overline{M}_n$ = number-average molecular weight defined by Equation (28)

$\overline{M}_w$ = weight-average molecular weight defined by Equation (29)

$N_{\max,1}$, $N_{\max,2}$, $N_{\max,3}$ as defined by Equations (75), (76), and (77), respectively

$\hat{N}_1$, $\hat{N}_2$, $\hat{N}_3$ as defined by Equations (95) to (97), respectively

N_{ij} = defined by Equation (74)

P = pressure

$\hat{P}$ = dimensionless maximum reactor temperature defined by Equation (86)

Pe_I = Peclet number for mass transfer of initiator defined as $vL/\hat{D}_I$

Pe_M = Peclet number for mass transfer of monomer defined as $vL/\hat{D}_M$

Pe_{M_r} = Peclet number for mass transfer of dead polymer of chain length r defined as $vL/\hat{D}_{M_r}$

Pe_H = Peclet number for heat transfer defined as $\rho v\, C_p L/\hat{K}_L$

Q_0, Q_1, Q_2 = the zeroth, first, and second moments of total dead polymer concentration defined by Equation (27)

Q_0^*, Q_1^*, Q_2^* = the zeroth, first, and second moments of total active polymer concentration defined as

$\sum_{r=1}^{\infty} C_{M_r^*}$, $\sum_{r=1}^{\infty} r\,C_{M_r^*}$ and $\sum_{r=1}^{\infty} r^2\,C_{M_r^*}$, respectively

R = gas constant

R^* = initiator free radicals

R_d = initiator decomposition reaction rate given by Equation (1)

R_i = chain initiation reaction rate given by Equation (2)

R_M = overall polymerization reaction rate given by Equation (3)

R_{M_r} = overall reaction rate for dead polymer of chain length r

T = reactor temperature

T_c = coolant temperature

T_0 = temperature of feed stream

U = overall heat transfer coefficient

v = linear velocity of the fluid in the reactor

x = axial distance in a tubular reactor

y_c = dimensionless coolant temperature defined as $(T_c - T_0)/\epsilon_1 T_0$

y_1 = dimensionless initiator concentration defined as $[(C_I)_0 - C_I]/(C_I)_0$

y_2 = dimensionless monomer concentration defined as $[(C_M)_0 - C_M]/(C_M)_0$

y_3 = dimensionless reactor temperature defined as $(T - T_0)/\epsilon_1 T_0$

y_4 = dimensionless total dead polymer concentration defined as

$$\left[\sum_{r=2}^{\infty} (C_{M_r})_0 - \sum_{r=2}^{\infty} C_{M_r}\right] \Bigg/ \sum_{r=2}^{\infty} (C_{M_r})_0 = [(C_4)_0 - Q_0]/(C_4)_0$$

y_5 = dimensionless first moment of the total dead polymer concentration defined as

$$\left[\sum_{r=2}^{\infty} (rC_{M_r})_0 - \sum_{r=2}^{\infty} (rC_{M_r})\right] \Bigg/ \sum_{r=2}^{\infty} (rC_{M_r})_0 = [(C_5)_0 - Q_1]/(C_5)_0$$

y_6 = dimensionless second moment of the total dead polymer concentration defined as

$$\left[\sum_{r=2}^{\infty} (r^2C_{M_r})_0 - \sum_{r=2}^{\infty} (r^2C_{M_r})\right] \Bigg/ \sum_{r=2}^{\infty} (r^2C_{M_r})_0 = [(C_6)_0 - Q_2]/(C_6)_0$$

$\hat{y}_1, \hat{y}_2 \ldots, \hat{y}_6$ defined by Equations (48) to (51), respectively

z = dimensionless distance defined by x/L

Greek Letters

α_1 = defined by Equation (91)

α_2 = defined by Equation (106)

β = defined by $4UL/\rho C_p v D$

ϵ = empirical constant for initiator efficiency

ϵ_1 defined by $1/(\hat{E}_d/RT_0)$

ϵ_2 defined as $\hat{E}_{pol}/\hat{E}_p$

ρ = density of fluid

ν as defined by Equation (8)

$\mu_1^I, \mu_1^{II}, \mu_1^{III}$ = largest eigenvalues as defined by Equations (92) to (94), respectively

LITERATURE CITED

Agrawal, S. C., "Use of Function Space Methods for the Analysis of Tubular Reactors with Axial Mixing," Ph.D. thesis, Polytechnic Institute of New York, Brooklyn (1974).

Albright, L. F., *Processes for Major Addition Type Plastics and their Monomers*, McGraw Hill, New York (1974).

Aris, R., *Introduction to the Analysis of Chemical Reactors*, Prentice-Hall, Inc., Englewood Cliffs, N. J. (1965).

Bamford, C. H., W. G. Barb, A. D. Jenkins, and P. F. Onyon, *The Kinetics of Vinyl Polymerization by Radical Mechanisms*, Academic Press, New York (1958).

Cintron-Cordero, R., R. A. Mostello, and J. A. Biesenberger, "Reactor Dynamics and Molecular Weight Distributions: Some Aspects of Continuous Polymerization in Tubular Reactors," *Can. J. Chem. Eng.*, **46**, 434 (1968).

Coddington, E. A., and N. Levinson, *Theory of Differential Equations*, McGraw-Hill, New York (1955).

Ehrlich, P., and R. N. Pittilo, "A Kinetic Study of the Oxygen-Initiated Polymerization of Ethylene," *J. Polym. Sci.*, **43**, 389 (1960).

———., and J. D. Cotman, "The Oxygen-Initiated Polymerization of Ethylene and the Oxidation of Ethylene at High Pressure," *J. Polym. Sci.*, **32**, 509 (1958).

Flory, P. J., *Principle of Polymer Chemistry*, Cornell Univ. Press, Ithaca, N. Y. (1953).

Friedman, B., *Principles and Techniques of Applied Mathematics*, Wiley, New York (1956).

Goldstein, R. P., and N. R. Amundson, "An Analysis of Chemical Reactor Stability and Control—Xa," *Chem. Eng. Sci.*, **20**, 195 (1965).

Goldstein, R., and C. S. Hwa, "Modeling and Analysis of Complex Reactors by Computer Simulation," paper presented at the Am. Chem. Soc. Symp. on Analysis of Complex Reaction System, Pittsburgh, Pa. (1966).

Guillet, J. E., T. R. Walker, M. F. Meyer, J. P. Halk, E. B. Towne, "Determination of Decomposition Rates of Diacyl Peroxides," *Ind. Eng. Chem. Process Design Develop.*, **4**, 257 (1964).

Han, C. D., and S. Agrawal, "Function Space Methods for Analysis of Nonadiabatic Tubular Reactors with Axial Mixing—1. Uniqueness Criteria of the Steady State and Computation of the Steady State Profiles," *Chem. Eng. Sci.*, **28**, 1617 (1973).

Hoftyzer, P. J., and Th.N. Zwietering, "The Characteristics of a Homogenized Reactor for the Polymerization of Ethylene," *ibid.*, **14**, 241 (1961).

Levenspiel, O., *Chemical Reaction Engineering*, Wiley, New York (1962).

Miles, D. C., and J. H. Briston, "Polymer Technology," *Chemical Publ. Co.*, New York (1965).

Mullikin, R. V., P. E. Parisot, and N. L. Hardwicke, "Analog Computer Studies of Polyethylene Reaction Kinetics," paper presented at the 58th AIChE Annual Meeting, Philadelphia (1965).

Raff., A. V. and J. B. Allison, *Polyethylene*, Interscience, New York (1956).

Shrier, A. L., B. F. Dodge, and R. H. Bretton, "Free-Radical Polymerization of Ethylene at High Pressures," paper presented at AIChE—Brit. Inst. of Ch.E. Joint Meeting (1965).

Smith, J. M., *Chemical Engineering Kinetics*, McGraw-Hill New York (1970).

Smith, M. V., *Manufacture of Plastics*, Reinhold, New York (1964).

Steiner, R., F. Wöhler, and K. Schoenemann, "Hochdruckpolymerisation von Aethylen mit Azo-bis-isobutyronitril als Initiator," *Chem. Eng. Sci.*, **22**, 537 (1967).

Thies, J., and K. Schoenemann, "The Calculation of High Pressure Polyethylene Reactors by Means of a Model Comprehending Molecular Weight Distribution and Branching of the Polymer," *1st Intern. Symp. Chem. React. Eng.*, Carnegie Inst., Washington, D. C. (1970).

Tobolsky, A. V., and R. B. Mesrobian, *Organic Peroxides*, Interscience, New York (1954).

Volter, B. V., "Study of Industrial Production of Polyethylene under High Pressures, and of the Automatic Control of the Process," paper presented at the Second Intern. Fed. of Automatic Control Congress, Basel (1963).

Warden, R. B., and N. R. Amundson, "Stability and Control of Addition Polymerization Reactions," *Chem. Eng. Sci.*, **17**, 725 (1962).

Zeman, R. J., and N. R. Amundson, "Continuous Polymerization Models—I. Polymerization in Continuous Stirred Tank Reactors," *Chem. Eng. Sci.*, **20**, 331 (1965).

Manuscript received August 14, 1974; revision received December 27, 1974, and accepted January 17, 1975.